Laser doppler anemometry study of reactant flow in fuel cell channels

A.Kucernak[a], Bradley Ladewig[a], Robert Blewitt[b], John Shrimpton[b]

[a] *Dept. of Chemistry, Faculty of Physical Science*
[b] *Dept. of Mechanical Engineering, Faculty of Engineering*
Imperial College London, SW7 2AZ London, UK

A.Kucernak@imperial.ac.uk, phone +44(20)759-45831, fax: +44(20)759-45801

Abstract

The flow pattern around a 180 degree turn in a square section 2mm gas channel of an optically accessible operating PEM fuel cell has been investigated using the non-invasive laser Doppler anemometry (LDA) technique. This approach involves 'seeding' the reactant gas (air) with water droplets ~2 µm in size, and measuring the velocity of these particles, Figure 1. The results reveal the symmetrical Ekman vortex pair expected to be present while operating at Reynolds and Dean numbers of 80 and 54, but also that additional complexity due to the combination of the operating MEA (membrane electrode assembly) and the abrupt change in wall direction. Measured velocities normal to and near the gas diffusion layer (GDL) surface were compared to expected velocities assuming pure diffusion, and found to exceed these diffusion velocities by several orders of magnitude implying that flow into the GDL is not inconsequential, contrary to the assumption made in many models.

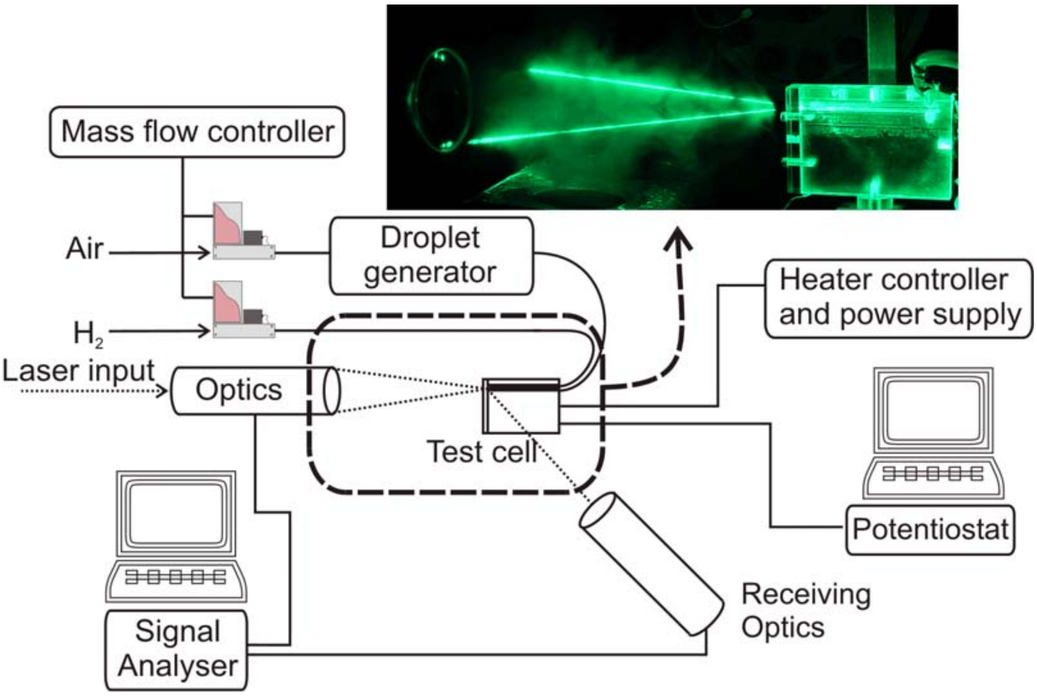

Figure 1. Experimental configuration for optical fuel cell with concurrent LDA measurement

Measuring and Modeling the Single Electrode Reactions in Polymer Electrolyte Fuel Cells

Holger Kuhn, Bernhard Andreaus, Alexander Wokaun, Günther G. Scherer

Paul Scherrer Institut, Electrochemistry Laboratory, 5232 Villigen, Switzerland

Electrochemical impedance spectroscopy (EIS) is a powerful tool to characterise polymer electrolyte fuel cells (PEFCs) and understand the electrochemical processes therein [1,2]. However, one has to bear in mind an important implication in interpreting the impedance spectra: due to the nature of the *solid* polymer electrolyte membrane one cannot easily introduce a reference electrode into the cell, as it is done with cells containing a liquid electrolyte, and therefore determine single electrode behaviour. Hence, integral impedance spectra, measured over the complete active area and across the entire cell do not allow detecting local processes neither at anode nor cathode.

We introduce a pseudo reference electrode into the solid electrolyte of a 1-dimensional cell [1], and therefore can separate the integral impedance of the cell into anode and cathode contributions. In particular, the anode impedance allows identifying different processes, which we attribute to the hydrogen adsorption, proton generation, and proton diffusion process, the latter includes water transport in the aqueous phase within the polymer morphology. A state-space model approach based on the kinetic reactions was applied, which allows for the determination of the kinetic parameters for these single reaction steps, which are not accessible by measuring the impedance across the entire cell [3].

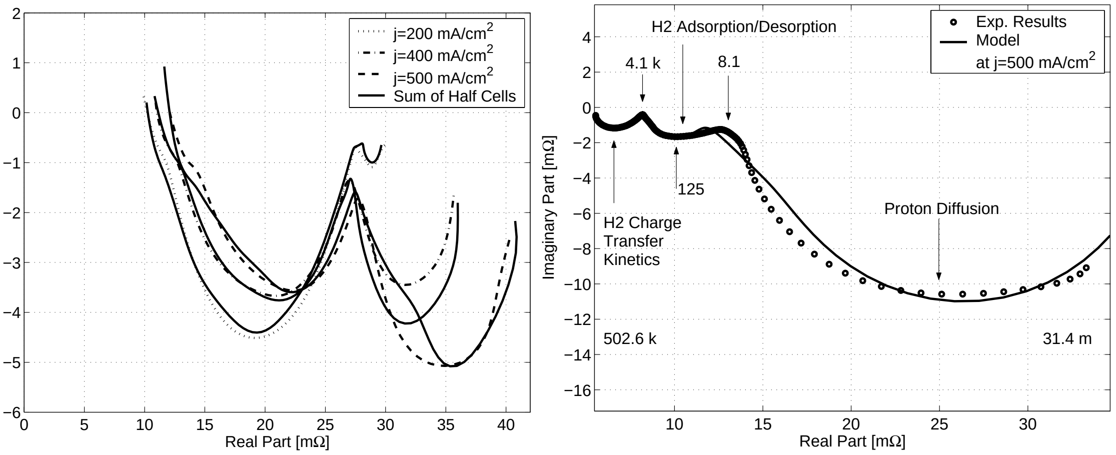

Fig 1: Left Figure: Comparison of the entire cell impedance with the sum of the half cell measurements. Right Figure: Comparison of the experimental data and the model evaluation of the hydrogen oxidation reaction (HOR) at j = 500 mA/cm2 (A = 28 cm^2). Different reaction steps of the HOR can be distinguished.

References

[1] B. Andreaus, A.J. McEvoy, G.G. Scherer, Electrochimica Acta 47 (2002) 2223
[2] B. Andreaus, G.G. Scherer, Solid State Ionics 168 (2004) 311
[3] H. Kuhn, B. Andreaus, A. Wokaun, G.G. Scherer, Electrochimica Acta, accepted

Direct methanol fuel cells modeling using standard proton exchange membranes properties

V.S. Silva[2], A. Mendes[2,*], L.M. Madeira[2] and S.P. Nunes[1]

[1] GKSS Research Centre, Max-Planck Str., 21502 Geesthacht, Germany

[2] LEPAE, Chemical Engineering Department, Faculty of Engineering, University of Porto, Rua Dr. Roberto Frias, 4200-465, Porto, Portugal

The proton exchange membrane (PEM) research plays an important role in the development of the fuel cell technology [1]. In the particular case of the direct methanol fuel cell (DMFC), the PEM should have a low permeability coefficient for the reactants (mainly methanol), and exhibit a high proton conductivity, along with long term mechanical stability [1]. Although perfluorinated membranes, such as Nafion®, are very suitable for hydrogen fuel cells, they have a strong drawback as far as DMFC application is concerned: the permeability towards methanol is high, leading to a significant efficiency reduction [2].

These problems can be mitigated by developing new materials, or modifying the existing ones, in order to prepare PEMs with improved properties compared to perfluorinated membranes. Usually, PEM researchers apply selected characterization methods such as impedance spectroscopy and pervaporation experiments in order to predict qualitatively the membrane performance in the DMFC [3,4]. Ideally, these membrane characteristics should be used as inputs in a mathematical model to quantitatively predict the corresponding DMFC output. However, up to nowadays most of the DMFC modeling research has focused extensively on Nafion® and most of the used parameters are obtained from literature [5]. These parameters in many cases hardly represent the properties of membranes under development limiting the usefulness and success of the model.

In order to provide a useful tool for predicting the DMFC performance when novel PEM materials are developed, a one-dimensional mathematical model is presented that enables the use of results evaluated through easy to implement characterization methods. The model development is based on membranes prepared with sulfonated poly(ether ether ketone) (sPEEK) polymer modified via *in-situ* incorporation of zirconium oxide [3]. The modeling of these membranes enabled the simulation of a DMFC for a wide variety of physical/chemical membrane properties.

The simulation curves and experimental points [4] for the current density-voltage and current density-power density plots using MEAs made from sPEEK composite membranes with 5.0, 7.5 and 10.0wt.% of ZrO_2 are shown in Fig. 1. From these plots, it can be seen that the model predicts accurately the performance of the DMFC using composite membranes with a wide range of properties concerning proton conductivity and barrier attributes [3], showing that the simulator can perform a useful first prediction of the DMFC performance, using the standard characterization data as model input parameters. The present model can also be used to answer many open questions regarding DMFC, especially in terms of which are the optimal PEM properties, having a compromise between proton conductance and methanol transport.

REFERENCES

---

[*] Corresponding author: Tel: +351 22 508 1695, Fax: +351 22 508 1449, e-mail: mendes@fe.up.pt

[1] L. Jörissen, V. Gogel, J. Kerres and J. Garche, New membranes for direct methanol fuel cells, J. Power Sources 105 (2002) 267.

[2] F. R. Kalhammer, P. R. Prokopius and V. P. Voecks, Status and prospects of fuel cells as automobile engines, State of California Air Resources Board, California, 1998.

[3] V.S. Silva, B. Ruffmann, H. Silva, Y. Alvarez, A. Mendes, L. M. Madeira and S. P. Nunes, Proton electrolyte membrane properties and direct methanol fuel cell performance, I Characterization of hybrid sulfonated poly(ether ether ketone)/zirconium oxide membranes, J. Power Sources 140 (2005) 34.

[4] V.S. Silva, J. Schirmer, R. Reissner, B. Ruffmann, H. Silva, A. Mendes, L. M. Madeira and S. P. Nunes, Polymer electrolyte membrane properties and direct methanol fuel cell performance, II Fuel cell performance and membrane properties effects, J. Power Sources 140 (2005) 41.

[5] K.Z. Yao, K. Karan, K.B. McAuley, P. Oosthuizen, B. Peppley and T.Xie, A review of mathematical models for hydrogen and direct methanol polymer electrolyte membanre fuel cells, Fuel Cells 4 (2004) 3.

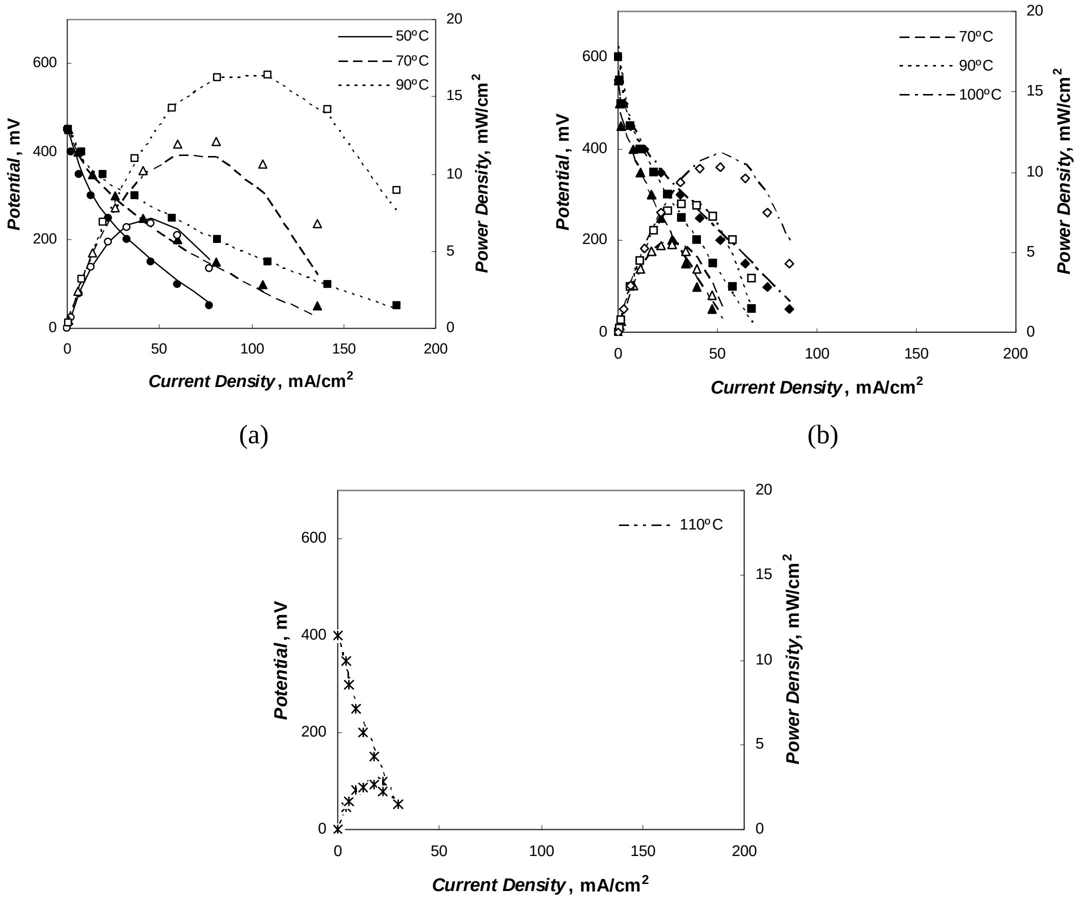

(a)

(b)

(c)

Fig. 1. Predicted (curves) and experimental (points: ● 50ºC; ▲70ºC; ■ 90ºC; ◆ 100ºC; ✳ 110ºC) current-voltage and power density plots for DMFC operation using sPEEK composite membranes with: a) 5.0, b) 7.5 and c) 10wt.%ZrO_2.

Quasi–2D semi–analytical models of a PEFC and DMFC

A.A.Kulikovsky
Institute for Materials and Processes in Energy Systems (IWV–3)
Research Center “Jülich”, D–52425 Jülich, Germany
On leave from
Moscow State University, Research Computing Center, 119992 Moscow, Russia

Introduction

Numerical models of a low–temperature fuel cells become more and more sophisticated; state–of–the–art models take into account minor details of transport and kinetic phenomena in a cell. The cost of detailed description is, however, a loss of clarity: 3D models usually involve a large number of poorly known parameters. Furthermore, these models are time–consuming and thus are hardly suitable for massive comparison of e.g. experimental and numerical polarization curves.

In this situation a simplified analytical models might bridge the gap between multi–dimensional modeling and experiment. Analytical models involve minimal number of parameters and are fast. They are ideally suited for rough characterization of cells in particular regimes, when the model assumptions are fulfilled. Moreover, these models predict new effects in cell functioning. In this work we review recent results in analytical modeling of a PEFC [1] and DMFC [2].

The models [1, 2] take into account consumption of feed gases as they move along the channel. The respective 1D mass balance equations are coupled by the equation of equipotentiality of cell electrodes, which accounts for the transport of reactants across the cell (including methanol crossover in DMFC). Both analytical models are, therefore, 1D+1D.

PEFC: regimes and optimal conditions

The model of a PEFC [1] includes the effects of oxygen depletion and accumulation of water in the cathode channel. The model predicts that the cell may operate in one of the three regimes: (i) water–limiting, when everywhere along the channel local current is limited by poor membrane humidification, (ii) oxygen–limiting, when local current is limited by the lack of oxygen and (iii) mixed: water–limiting close to the channel inlet and oxygen–limiting in the rest part of the cell. In the latter regime local current density exhibits maximum [1b].

In the limit of low cell voltage the model gives analytical expressions for along–the–channel profiles of local current density $j(z)$ and of oxygen and water concentrations. In case of arbitrary cell voltage the problem reduces to the system of two ODE's. Numerical solution of this system is easy, fast and can be used as a part of fitting algorithm. The resulted profiles of $j(z)$ are in good agreement with recent experiments.

The model gives expressions for optimal feed composition and oxygen stoichiometry. Experimental verification of these predictions is in progress in our Institute.

DMFC: the bridge

1D+1D model of DMFC reveals a new effect. When mean current density in a cell J tends to zero, a narrow current–carrying domain (bridge) forms at the inlet of the cathode channel. Analysis shows that localization of current close to the channel inlet occurs due to lack of oxygen in the rest part of the cell [2]. The bridge short–circuits the electrodes, thus reducing cell open–circuit voltage. The bridge arises only in the cell with crossover; in the case of zero crossover the effect disappears. This effect explains a well–known phenomenon of mixedpotential in a DMFC.

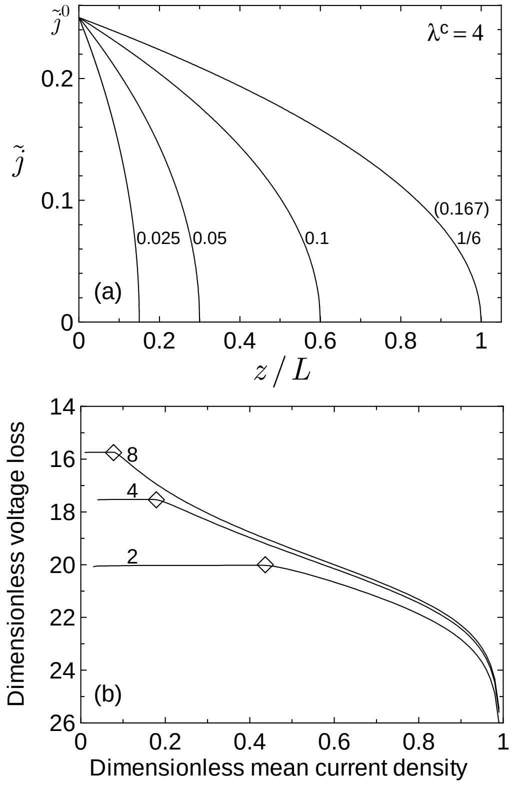

Figure 1: (a) The shape of dimensionless local current density ($\tilde{z} = z/L$ is coordinate along the channel) for indicated values of dimensionless mean current density $\tilde{J}$ in a cell. (b) Voltage loss vs. mean current density (cell polarization curve) for indicated values of oxygen stoichiometry.

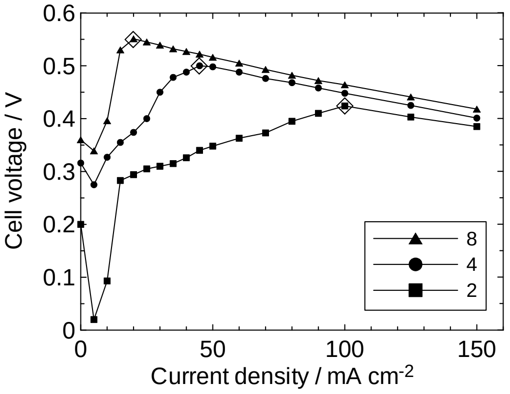

Figure 2: Experimental polarization curves of DMFC for indicated values of oxygen stoichiometry. Diamonds – the points, where the bridge forms (cf. Figure 1b).

Furthermore, as J drops down below critical value J_0, local current density at the channel inlet j^0 ceases to change (Figure 1a). Further decrease in J is provided by bridge "shrinking" (Figure 1a). Constant j^0 induces constant overpotentials on both sides of the cell. The bridge, therefore, manifests itself as a plateau on the cell polarization curve in the region of small currents (Figure 1b). Diamonds in Figure 1b indicate the points, where the bridge forms ($j(L) = 0$, L is the channel length).

To verify these predictions we have measured DMFC polarization curves in the conditions, which correspond to the model assumptions. The results of the measurements [3] are shown in Figure 2. Comparing Figures 2 and 1b we see that the experimental curves remarkably well reproduce two main features of the model curves: the drastic change in the slope at the critical current density J_0 (diamonds in Figures 2 and 1b) and the decrease of J_0 with the increase in oxygen stoichiometry λ^c. Furthermore, the ratio of J_0's for $\lambda^c = 8$, 4 and 2 in Figure 2 is very close to this ratio for the model curves in Figure 1b. For $J \leq J_0$ model predicts constant cell voltage (Figure 1b); the experimental curves, however, exhibit decrease in cell voltage to the left of J_0 (Figure 2). This suggests that in the real cell the effect is even stronger and j^0 increases as $J \to 0$.

This may occur due to the non-uniform flooding of the cathode catalyst layer. If the bridge shrinks faster, than prescribed by the model, j^0 must increase in order to provide the required total current in a cell. The increase in j^0 leads to the decrease in cell voltage. A more detailed picture of the bridge will give measurements of local current, which are in progress.

References

[1] A. A. Kulikovsky. *Electrochimica Acta*, **49** (2004) 5187; *Electrochem. Comm.*, **6** (2004) 969.

[2] A. A. Kulikovsky. *Electrochem. Comm.*, **6** (2004)1259; *J. Electrochem. Soc.*, (submitted).

[3] A. A. Kulikovsky, K.Klafki, K.Wippermann. *Electrochem. Solid–State Lett.*, (submitted).

THREE-DIMENSIONAL, MULTI-PHASE MODEL OF THE GAS DIFFUSION ELECTRODES IN A PEM FUEL CELL

Torsten Berning
Adam Opel AG- GM Fuel Cell Activities
International Technical Development Center

In order to further improve the performance of a PEM Fuel Cell numerous computational models have been devised in the past to shed insight in the various transport phenomena that occur during fuel cell operation. These models have become more increasingly more sophisticated, moving from one- and two-dimensional, single phase models [1-3] towards two- and three-dimensional, multi-phase models [4-6]. A three-dimensional, two-phase model of a PEM fuel cell, however, has not been presented, yet. This paper describes the numerical model that has been developed at the University of Victoria during recent years. Employing the methods of computational fluid dynamics, and building on a 3D single-phase model [7] we have implemented a multi-phase model into the commercial software code CFX 4. Altogether, the model accounts for multi-phase, multi-component transport in porous media with electrochemical reactions and heat transfer. Transport of liquid water is described via Darcy's law and a capillary pressure in conjunction with the Leverett's equation to describe the capillary pressure function. Both anode and cathode are included. A binary gas mixture of hydrogen and water vapour is considered at the anode and humidified air at the cathode. Figure 1 shows the distribution of the liquid water saturation in both gas diffusion electrodes. Under the conditions investigated, there is a significant amount of liquid water not only in the cathode side but at the anode side as well. This is due to the fact that when fully saturated hydrogen enters the cell, the consumption of the reactants lead to an oversaturation, since the molar fraction of water vapour increases. This leads to condensation inside the GDEs. The condensation water is dragged along with the gas phase towards the catalyst layer, and can only leave the cell via the build-up of a capillary pressure gradient, which drives the water out of the cell. Figure 2 shows the development of the average liquid water saturation in the gas diffusion layers with current density. Overall, the saturation levels are of the same order as those reported by Wang *et al.* [4]. The drop-off of the liquid water saturation in the cathode at a high current density can be explained by the higher fraction of the total current being generated under the channel area [7], which reduces the diffusion path of the water out of the cell. At the same time, the rate of evaporation increases, as is shown in Figure 3. The direction of phase change inside the GDE is governed by the relative humidity. Three different underlying mechanisms of phase change have been identified: i.) an increase in temperature due to the electrochemcial reaction leads to an increase in the saturation pressure, causing evaporation in the presence of liquid water; ii.) the pressure drop inside the GDE (Darcy’s law) leads to a decrease in the partial pressure of water vapour and causes evaporation as well; iii.) the consumption of reactants leads to an increase in the molar fraction of water vapour, which causes condensation. The second effect is strongly controlled by the properties of the GDE, especially the hydraulic permeability. A high permeability leads to a reduced pressure drop and causes less evaporation.

References:

[1] T. E. Springer , T. A. Zawodzinski and S. Gottesfeld: *J. Electrochem. Soc.*, Vol. 138, No. 8, 1991.

[2] D. M. Bernardi and M. W. Verbrugge, *J. Electrochem. Soc.*, Vol. 139, No. 9, 1992.

[3] T. V. Nguyen and R. E. White, *J. Electrochem. Soc*., Vol. 140, No. 8, 1993.

[4] Z. H. Wang , C. Y. Wang and K. S. Chen, *J. Power Sources*, Vol. 94, 40-50, 2001.

[5] D. Natarajan and T.V.Nguyen, *J. Electrochem. Soc*., Vol. 148, No. 12, 2001.

[6] S. Dutta, S. Shimpalee and J.W Van Zee, *J. Applied Electrochem.*, Vol. 30, 135-146, 2000.

[7] T. Berning, D. Lu and N. Djilali, *J. Power Sources*, Vol. 45, No. 11, 2002.

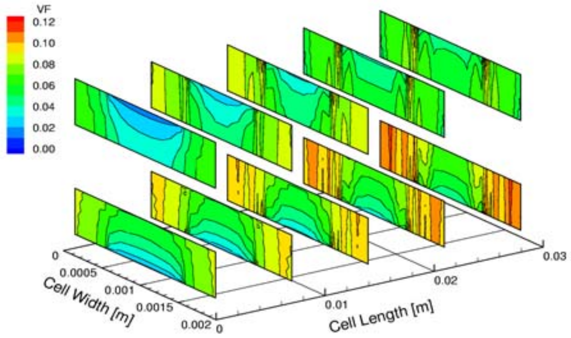

Fig. 1: Liquid water saturation inside the cathodic (lower) and anodic (upper) GDE. The channel interface area lies between 0.5 mm and 1.5 mm.

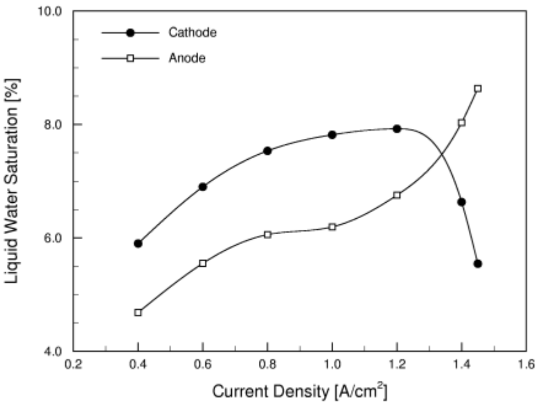

Fig. 2: Average liquid water saturation in the gas diffusion electrodes. The limiting current density is 1.5 A/cm^2, and is governed by the oxygen diffusion limitation.

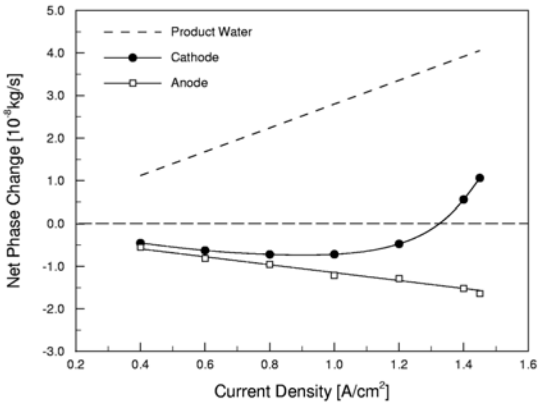

Fig. 3: Overall amount of phase change in the gas diffusion electrodes. The zero line indicates that, on average, the same amount of water vapour leaves the cell as enters, whereas positive values indicate that, overall, product water evaporates.

Modelling of PEFC and SOFC using Electrochemical Impedance Spectroscopy (EIS)

Norbert Wagner, Deutsches Zentrum für Luft- und Raumfahrt
Pfaffenwaldring 38-40 - 70569 Stuttgart, Germany
Tel +49 711 6862 631 - Fax +49 711 6862 322
norbert.wagner@dlr.de

The need for an efficient, non-polluting power source for vehicles in urban environments, emphasised by legislative initiatives, has resulted in increased attention to the option of fuel-cell-powered vehicles of high efficiency and low emissions. Recently, fuel cells are also used in a variety of new applications like portable devices (e.g. radio communication, mobile phones, lap-tops, etc.), residential applications (combined heat and power generation) and other transport applications (e.g. submarines, ships, rail guided vehicles, etc.).

Both electrodes of a fuel cell (cathode and anode) are porous: porosity is needed in order to facilitate mass transport as well as to increase the reaction area and thereby improve current density. The important issues in the optimization of the electrodes are the stability of the porous structure and the maximization of the three-phase interface between the electrolyte, the gaseous (liquid) reactant and the electronically conducting catalyst in the electrode. Other R&D challenges are the investigation of the reaction mechanism and kinetic at each electrode/electrolyte interface, determination of degradation (poisoning) mechanism, production of cheap and efficient electrodes with low catalyst loading, development of suitable catalysts, long term stability, etc. In order to improve the efficiency as well as the reliability of the fuel cell systematically a better understanding of the electrochemical reactions and mass transport in the fuel cell is essential. Moreover, quality control and understanding of degradation require new non-destructive methods and a better understanding of experimental results based on modelling and simulation. However, EIS [1] is a versatile *in situ* investigation method which is increasingly applied in fuel cell research and development.

With the help of the EIS, it is possible to obtain information about the system with minimal external influences, directly “in situ“ in a running cell, up to a current of 100 A (for example using the electronic load EL101 from Zahner-elektrik). Even after the measurement, the cell can work at the same operation point. The AC response of the fuel cell provides additional information on the investigated system. The analysis of the impedance spectra involves the description of the system specific physical parameters of the electrochemical set up with an equivalent circuit. Ideally, it is then possible to separate the individual voltage losses of the single components, namely of the anode, cathode, electrolyte and perhaps even to identify diffusion processes to draw conclusions about the limiting processes which determine the performance of the fuel cell.

Starting with EIS measured with symmetrical gas supply, an equivalent circuit for the complete PEFC (SOFC) can be applied for the simulation of the measured impedance spectra of the PEFC. Besides a series resistance R_{el}, the equivalent circuit (Fig.1) contains 3 time constants of parallel R/C. In the simulation the capacitance (C) was replaced by CPE (CPE= constant phase element) due to the porous structure of the electrodes. The cathode can be described using a time constant for the charge transfer through the double layer ($R_{ct(C)}$ / $CPE_{dl(C)}$), a time constant for the finite diffusion of water with a Nernst-impedance like behaviour ($R_{(N)}$ / $CPE_{(N)}$ and finally the time constant of the anode ($R_{ct(A)}$ / $CPE_{dl(A)}$, the exponent of the CPE is around 0.80). Anode and cathode can be also simulated with the porous electrode model.

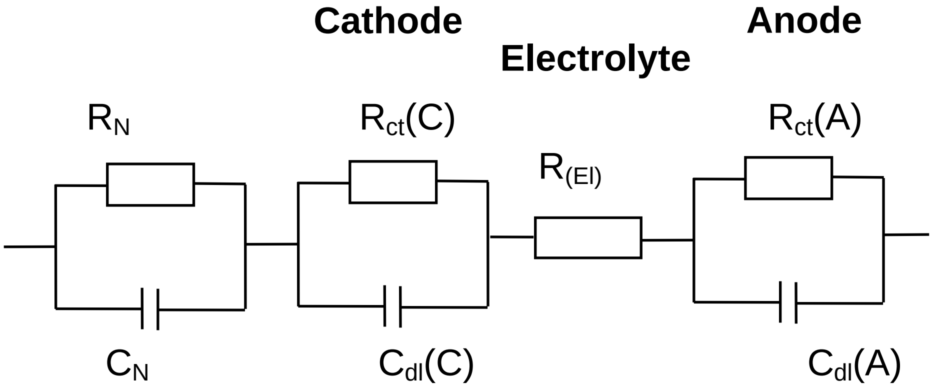

Fig.1: Equivalent circuit of the PEFC with O_2/H_2 gas supply, for high current densities with an additional diffusion step (Nernst-impedance)

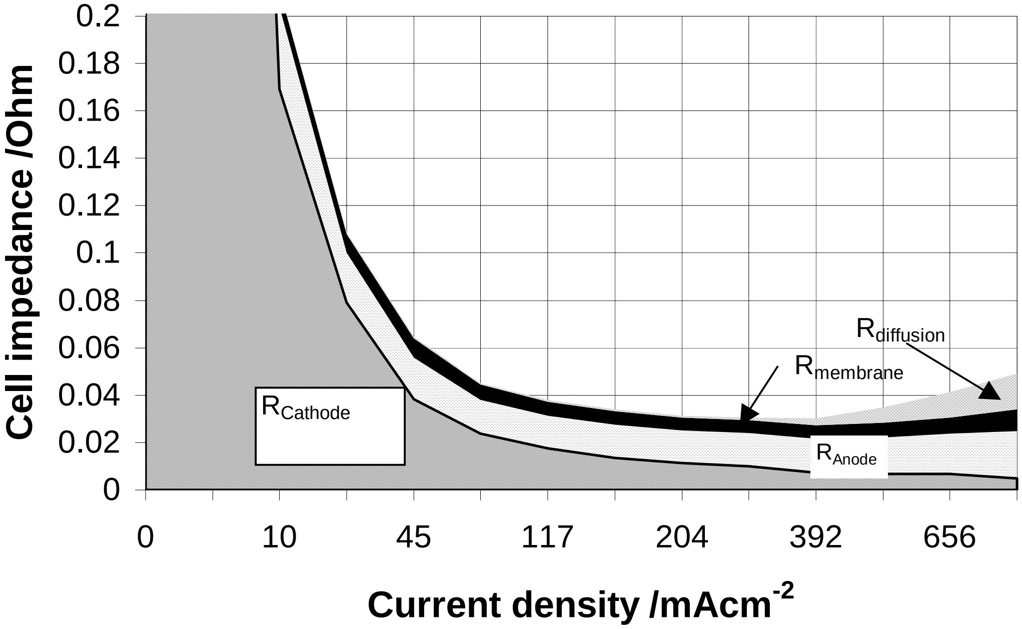

Fig. 2: Current density dependency of the resistances after evaluation of the impedance spectra evaluated with EC from Fig. 1

Literature

1. N. Wagner, "Electrochemical power sources – Fuel cells" in *Impedance Spectroscopy: Theory, Experiment, and Applications*, 2nd Edition, Edited by Evgenij Barsoukov and J. Ross Macdonald, John Wiley&Sons, Inc., ISBN: 0-471-64749-7, March 2005 (in press)

Fast Locally Resolved Electrochemical Impedance Spectroscopy in Polymer Electrolyte Fuel Cells

I.A. Schneider, A. Wokaun, G.G. Scherer
Electrochemistry Laboratory
Paul Scherrer Institut
5232 Villigen PSI, Switzerland

The overall performance of a polymer electrolyte fuel cell is determined by a complex interplay of elementary processes, i.e. kinetics, ionic, and electronic conductivity of membrane and catalyst layers as well as mass transport. Transient methods such as electrochemical impedance spectroscopy (EIS) can be used to separate electric, kinetic, and diffusion processes in an operating PEFC. However, inhomogeneities in fuel cells due to locally changing humidity, reactant concentration, temperature, etc. and thus inhomogeneities in local cell impedance and performance are highly likely to occur.

Therefore, spatially resolved *in situ* diagnostic methods for PEFCs are badly needed not only for measuring, but particularly for explaining local fuel cell performance. This type of detailed *in situ* diagnostics on a local scale will help to gain a detailed understanding of the processes limiting the performance of an operating PEFC and to validate computational fuel cell predictive models.

Therefore, we have developed a system for performing locally resolved EIS in a segmented PEFC [1]. The impedance measurement is performed for all segments in parallel. Due to this unique fast parallel approach the measurement period for obtaining a locally resolved impedance spectrum is virtually independent of the number of segments used in a segmented PEFC. For our measurements shown in Fig. 1 we have been using a PEFC (area 29,2 cm^2) with a nine-fold segmented serpentine cathode flow field and an unsegmented serpentine anode flow-field.

Locally resolved impedance spectra and the corresponding current density distributions have been taken in a segmented PEFC operated on H_2/O_2 and H_2/air. The results we obtained under low humidity reaction conditions for co- and counter flow in a PEFC operated on H_2/O_2 are shown here exemplarily (Figure 1).

When switching the reactant feed from counter- to co-flow mode the overall cell voltage strongly decreases from 651 mV to 482 mV (galvanostatic mode @ $I_{\mathrm{Cell}} = 14.6$ A). The differences in performance are reflected in variations in the current density distribution and the respective locally resolved impedance spectrum. In co-flow the current density increases with increasing humidity (Figure 1a), whereas in counter-flow mode the current density shows a maximum with a strong decreasing value at the O_2 inlet (Figure 1d).

In co-flow mode the shape of the local impedance spectrum changes dramatically along the channel (Figure 1b), i.e. the processes limiting cell performance change along the channel. According to our model [2] there are two kinetic regimes in the cell. At high current densities and high humidity (seg. 1-3) the ORR kinetics and the diffusion at the anode are rate limiting (Figure 1c). At low current densities and low humidity (seg. 6-9) the diffusion is less or not important, since the capacitive arc in the lower frequency range disappears and the inductive behaviour of the cathode [2] becomes dominating (Figure 1b). Here the ORR and, due to the formation of a third higher frequency arc, evenmore the HOR are limiting. The ohmic and especially the charge transfer resistance increase dramatically along the channel length with decreasing humidity due to drying of the membrane and the catalyst layers (Figure 1b).

A higher frequency third arc is also seen in the spectrum of seg.1 (hydrogen inlet) in counter-flow mode (Figure 1f). Due to diffusion of water from the cathode to the anode this third arc disappears. Seg. 2, 3 and 4 (Figure 1f) show only one higher frequency cathodic arc. The charge transfer and ohmic resistance decrease with increasing current density. Segment 4 has the lowest charge transfer and ohmic resistance at all. The strong performance loss at the oxygen inlet (seg. 9) can be attributed to drying of the cathode catalyst layer and the membrane (Figure 1e), since oxygen is fed dry. Starting at the oxygen inlet, due to the formation of water on the cathode side and diffusion of water from anode to cathode the charge transfer and ohmic resistance rapidly decrease.

A variety of locally resolved impedance spectra and the respective current density distributions obtained under H_2/O_2 and H_2/air operation will be discussed in the presentation.

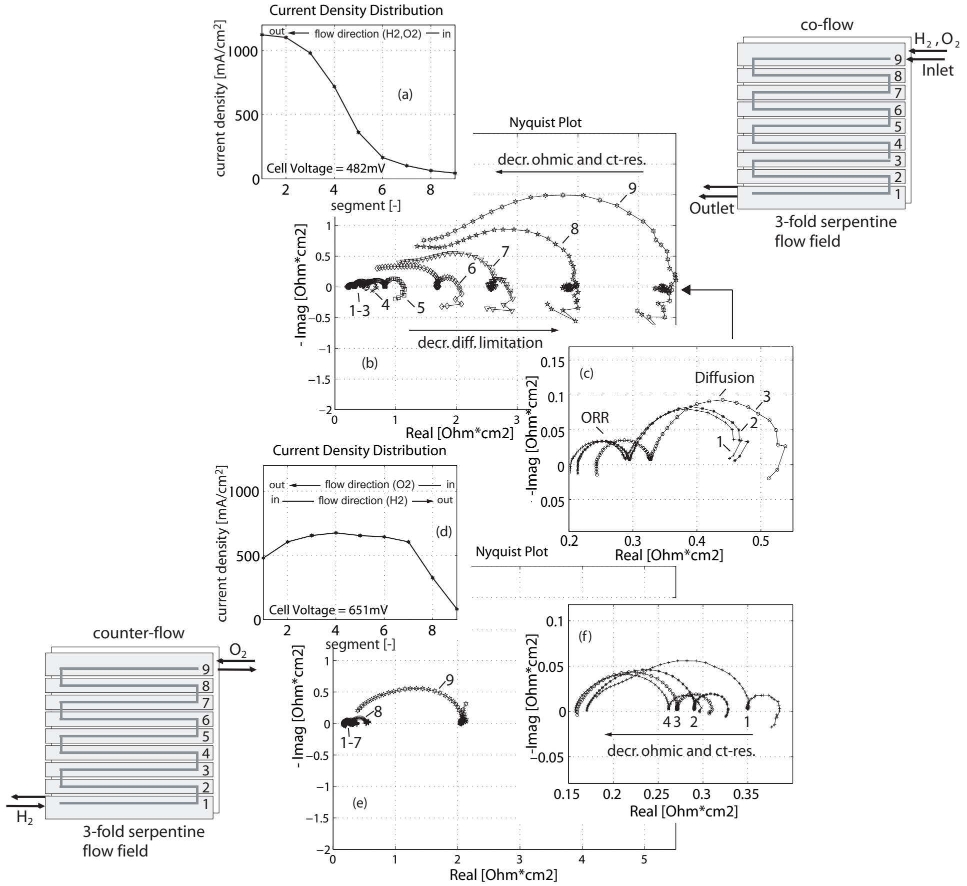

Figure 1: Locally resolved impedance spectra and respective current density distribution for a PEFC operated on pure H_2/O_2 in co- (Fig. 1a-c) and counter-flow (Fig. 1d-f) mode: MEA: Nafion 115, Pt/C electrodes 0.66 mg/cm^2; gases: $T_{H2} = T_{O2}$ = 70°C, r.h.(H_2) = r.h.(O_2) = 50%; stoich. (H_2) = stoich. (O_2) = 1.5; cell: ambient pressure, T_{Cell} = 70 °C; modulation frequency range from 0.0158 Hz to 10kHz.

[1] I.A. Schneider, H. Kuhn, A. Wokaun, G.G. Scherer, Proc. of the 4th Intl. Symp. on PEFCs, 206th ECS Meeting, Honolulu, Hawaii, Proc. (2004), to be published
[2] H. Kuhn, B. Andreaus, A. Wokaun, G.G. Scherer, Electrochim. Acta, accepted 2004

Transient numerical simulation of electrochemical dynamics: A new approach for fuel cell impedance calculations

Stefan Gewies, Wolfgang G. Bessler
Interdisciplinary Center for Scientific Computing, Heidelberg University
Im Neuenheimer Feld 368, 69120 Heidelberg, Germany

Summary. A new computational approach for simulating impedance spectra and polarization curves of electrochemical systems from detailed physicochemical models is presented. It is based on transient numerical simulations (TNS) of the dynamics of the system when a periodic variation of overpotential is imposed. Impedance is calculated in the time domain maintaining the full nonlinearity of the system. Polarization curves are obtained from the steady-state behavior. We show application of the method to SOFC Ni/YSZ pattern and cermet anodes operated with H_2/H_2O based on detailed models of surface electrochemistry, diffusive porous gas-phase transport, and electronic/ionic conductivity of metal and electrolyte.

Background. Electrical impedance spectra are commonly interpreted using equivalent circuit models [1]. Equivalent circuits, however, allow only limited insight into to the physicochemical properties of the system, not only due their ambiguity, but also because of their global nature. They furthermore do not allow the prediction of polarization curves.

Realistic SOFC models need to include detailed chemistry (rate equation description of chemical and charge-transfer reactions) and transport processes (fluid-dynamical description of convection and diffusion). CFD-type models have been employed on a cell-level scale, however applying simplified, global descriptions of electrode processes only. They can be used for predicting polarization curves, but are not able to simulate impedance.

Even if detailed-chemistry models are available, impedance simulations require the use of elaborate numerical algorithms. Gauckler and co-workers have successfully used state-space modelling (SSM) for impedance simulations of SOFC cathodes and anodes [2,3]. Their method is based on linearization of the governing equations, subsequent Laplace transformation, and impedance calculation in the frequency domain.

Approach. We present and apply an approach based on transient numerical simulation (TNS) of the governing equations [4,5], where impedance is calculated in the time domain maintaining the full nonlinearity of the system. Polarization curves are obtained from the steady-state behavior. The approach is based on the following scheme [5]:

(1) The reaction and diffusion processes in solid oxide fuel cells are described in the form of differential equations. These equations contain derivatives of the state variables (species concentrations, overpotential η, current density) with time and space.

(2) A harmonically varying overpotential is imposed to the system as boundary condition:

$$\eta(t) = \eta_{\text{steady}} + \eta_{\text{var}} \sin(\varpi t)$$

For calculating the steady-state polarization, η_{var} is set to zero.

(3) The equation system is time-integrated for one or several periods $\tau = 1/\omega$. This requires efficient numerical methods that can handle the stiff equation system and the boundary condition. We use the implicit extrapolation solver LIMEX [6]. Integration yields the transient be-

havior of all state variables including the Faradaic current $i(t)$ within the simulated time periods.

(4) The calculation of impedance from $i(t)$ given $\eta(t)$ is straightforward following the algorithms used in frequency response analysers [1].

SOFC Ni/YSZ anodes. Pattern anodes operated with H_2/H_2O are modelled using the six-step surface reaction mechanism proposed by Bieberle and Gauckler [3]. The mechanism includes charge-transfer, surface chemical reactions, and adsorption/desorption reactions. A sensitivity analysis of the model parameters on simulated polarization resistance allows the assessment of rate-controlling steps. Simulated impedance spectra at open circuit voltage show good agreement with experimental data (see Figure).

SOFC cermet anodes are modelled in 1D by coupling the surface electrochemistry model used for pattern anodes with a porous gas-phase diffusion model (Stefan-Maxwell law) and an electric/ionic conductivity model (Ohm's law). Simulations predict a strong local variation of the state variables (overpotential, gas-phase concentrations, surface coverages) along the anode thickness. Simulated impedance spectra reproduce typical features of experimental data.

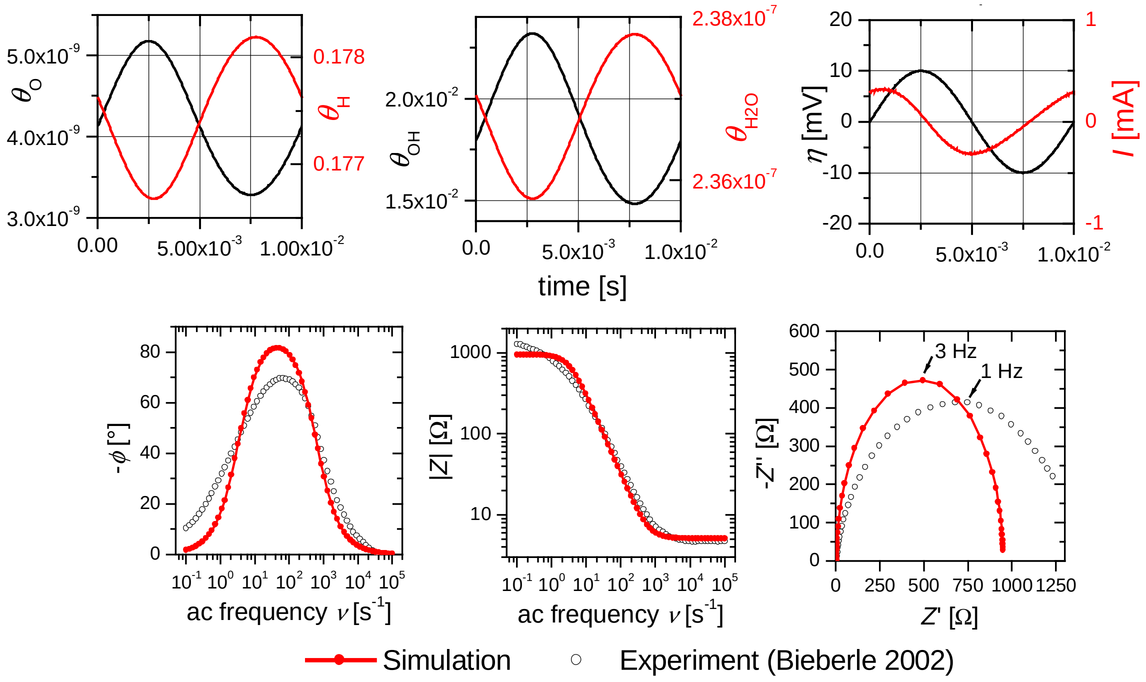

Pattern anode simulations: Transient behavior (100 Hz excitation) of state variables (surface coverages θ, *overpontential* η, *and Faradaic current* I*) and impedance spectra*

1. J. R. MacDonald, ed. *Impedance spectroscopy. Emphasizing solid materials and systems* (John Wiley&Sons, New York, 1987).
2. A. Mitterdorfer and L. J. Gauckler, *Solid State Ionics* **117** (1999) p. 187.
3. A. Bieberle and L. J. Gauckler, *Solid State Ionics* **146** (2002) p. 23.
4. W. G. Bessler and J. Warnatz, *Proceedings of the 6th European SOFC Forum* (Lucerne, Switzerland, 2004), p. 754.
5. W. G. Bessler, *Solid State Ionics* (2004), submitted.
6. P. Deuflhard, E. Hairer and J. Zugck, *Num. Math.* **51** (1987) p. 501.

Oxygen Diffusion and Temperature in Small Fuel Cell Stacks

G. Schlumberger*, O. Bender, L. Jörissen
ZSW, Center for Solar Energy and Hydrogen Research Baden Württemberg, Div. 3: Electrochemical Energy Storage and Energy Conversion,
89081 Ulm, Germany

Mini Fuel Cell Stacks up to 20 W have to work without peripheral devices, so it is not possible to control the oxygen input, the temperature of the Stack or the Cell Humidity during Operation. Instead, Stack architecture and Cell geometry have to be chosen like this, that a Stack can be operated without peripheral control sufficiently stable under a wide range of conditions.

The possible peak power of Ministacks is limited by a heavily climbing Stack temperature and rapidly falling O_2 - concentration in the cell air channels with increasing current density.
A stable long time operation of a Ministack is only possible if the cells have a certain humidity. The humidity depends strongly on e.g. Stack temperature and cross section of the air channels.

For the design of Mini Fuel Cell Stacks it is necessary to develop some mathematical models to predict their performance for desired applications. These Models should describe:

- the dependence of O_2 - concentration and maximal current density from cell geometry.
- the dependence of Stack temperature from Stack architecture.
- the dependence of Cell humidity from Cell geometry (including GDL - porosity).

The work presented here shows first results in the development and the experimental validation of simple analytic models on O_2 and temperature distribution in cylindrical Ministacks.

The first model, describing the O_2 - concentration in side channels and the dependency of the current density from the channel geometry, has been confirmed by experimental results (s. Diagram 1).

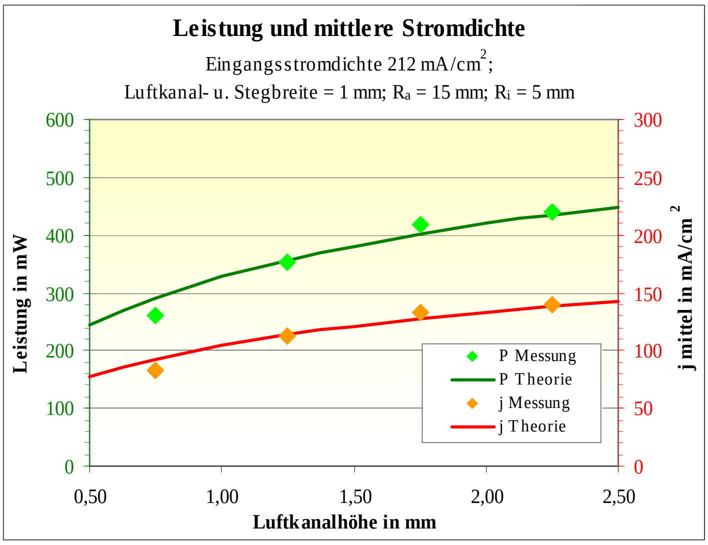

Diagram 1: O2 - Diffusion - Model and measured values for cylindrical Ministacks

The second model is estimating the Stack temperature in dependence of Stack architecture, Cell voltages and electrical current. The model is still in progress, but comparison with first experimental results indicate, that we are on the right way (s. Diagram 2).

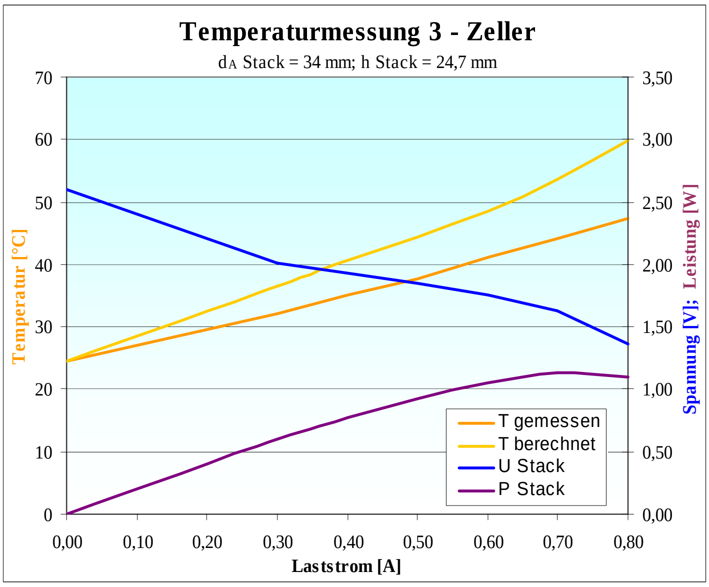

Diagram 2: Temperature - Model and measured values

Investigation of two-phase flow phenomena in polymer electrolyte fuel cells by neutron imaging

Denis Kramer[1], Jianbo Zhang[2], Eberhard Lehmann[3], Alexander Wokaun[1],
Kazuhiko Shinohara[2], Günther G. Scherer[1]

[1]Paul Scherrer Institut, General Energy Departement, Electrochemistry Laboratory, CH-5242 Villigen, Switzerland
[2]Nissan Motor Co. Ltd., Technology Research Laboratory No. 2, Nissan Research Center, 1 Natsushima-cho, Yokosuka 237-8523, Japan
[3]Paul Scherer Institut, Condensed Matter Research with Neutrons and Muons, ASQ Division, CH-5242 Villigen, Switzerland

The PEFC operates in a temperature regime below or slightly above 100°C and at near ambient pressure. Therefore, reaction water is likely to condense within the porous structures and flow distributors of a PEFC. The formation of a liquid phase might impede the transport of the educts (oxygen and hydrogen) to the catalytic active electrodes, and therefore limit electrical power density and efficiency.

Due to the high cross-section of hydrogen nuclei for neutrons, neutron imaging allows the non-invasive detection of liquid water within a fuel cell with reasonable spatial and temporal resolution. Appropriate data treatment allows quantitative analysis, which enables the correlation of liquid accumulation in gas diffusion layers and flow fields and electrochemical characteristics. In particular, correlations can be established with locally resolved current measurements.

The possibilities and limitations of the method discussed, algorithms for an enhanced quantitative evaluation presented, and their application to the data demonstrated. Results from PEFC investigations will be presented, which can serve as input data for modeling purposes.

References:

[1] D. Kramer et al., Electrochimica Acta, in press.
[2] D. Kramer et al., Nucl. Instrum. Meth. A, accepted.
[3] A. Geiger et al., Fuel Cells 2 (2) (2002) 92.
[4] D. Kramer et al., PSI Scientific Report, vol. 5, 2004, ISSN-1423-7342.

SOFC repeat element model validation by benchmarking and experiments

Diego Larrain, Jan Van herle, François Maréchal, Daniel Favrat
Lab. of Industrial Energy Systems (LENI), Institute of Energy Sciences,
Faculty of Engineering. Ecole Polytechnique Fédérale de Lausanne (EPFL).
CH-1015 Lausanne, Switzerland.

Introduction

The repeat element model developed in this work aims to be used as a versatile design tool to explore design solutions, perform sensitivity analysis and optimization. Validation of the model by benchmarking and experimental results comparison is presented.

Model benchmarking

The main model developed, which is a 2D model [1] is based on some assumptions that makes it efficient in terms of computational time. To validate the assumptions made and ensure the intrinsic validity of the model, benchmarking with a CFD model has been performed [2].
The output of the model are compared in the simulation of i-V characteristics, comparing temperatures, power outputs. Benchmarking has been performed as well on sensitivity to some geometrical variables and some operating variables.

Experimental validation

The configuration on which the model has been developed is tested experimentally, and a comparison and validation procedure has been setup. The i-V characteristics obtained, as well as the validation carried out from specific experiments are presented.

Global performance validation

Data from experiments are useful to modelers, however, several problem arises. Experimental reproducibility often represents a problem, and tests are often submitted to non-perfect behavior (leakages for example). From standard tests, the behavior of the repeat element or stack can be verified, for example the change in behavior with fluxes and temperature. If a major deviation, or a systematic deviation is found, this can be explained by a phenomena which is not accounted for in the model.
For example, in our case, the OCVs simulated were much higher than the experimentally obtained. A non-perfect behavior of the electrolyte has been introduced in the model and better OCV simulation are obtained (see in [1]).

Validation with local measurements

As standard experiment only gives the total current, the cell potential and eventually some temperatures (between 1 to 4 thermocouples), the information provided is not sufficient to validate the temperature field or current density field computed by the models. Specific experiments were carried out to measure local current densities and potential (segmented repeat element), and local temperature (with up to 20 thermocouples). Results from the experiments and from the model validation procedure are presented.

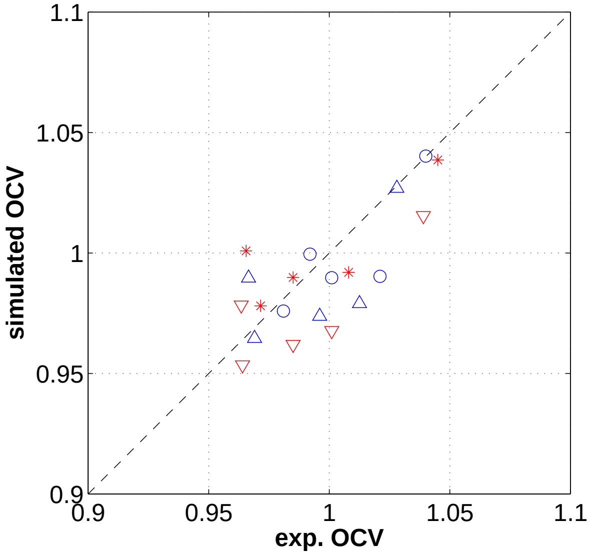

Figure 1: Local OCV comparison between the experimental data from a segmented repeat element and simulation

Local current density measurement allowed for example to validate the flow field and current/potential distribution on the repeat element for several operating points. Figure 1 reports the OCV comparison on the segments for 4 operating points. Most of the values are close, however, for one of the segments, but the error is much than in others. This suggests that the model does not represent accurately this part of the repeat element.

On figure 2, the variation of temperature for 2 thermocouples (one close to the fuel inlet and the other close to the post-combustion zone at the fuel outlet) is reported, as well as the simulated values. These results, though preliminary, show that the trend on both locations is well simulated.

For both experiments, parameter estimation is used to calibrate some uncertain model parameters. The discrepancies observed can lead to a modification of the model in order to improve the quality of the output.

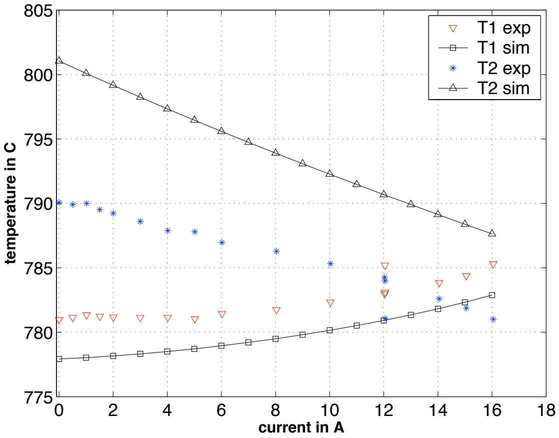

Figure 2: Local temperature, measured and simulated values (preliminary results)

Conclusion

The modeling approach, based on a simple model, is validated by benchmarking and experimental comparison. The validation procedure has allowed a significant improvement in the model results. The model can therefore be used with more confidence for sensitivity analysis and optimization.

References

[1] D. Larrain, J. Van herle, F. Maréchal, and D. Favrat. Generalized model of planar SOFC repeat element for design optimization. *J. of Power Sources*, 1-2(131):304–312, 2004.

[2] Diego Larrain, François Maréchal, Nordahl Autissier, Jan Van herle, and Daniel Favrat. Multi-scale modeling methodology for computer aided design of a solid oxide fuel cell stack. In A. Barbosa-Povoa and H. Matos., editors, *European Symposium on Computer Aided Process Engineering-14*, pages 1081–1086, 2004.

Proceedings
2nd Fuel Cell Research Symposium - Modelling and Experimental Validation
March 3-4, 2005, Stuttgart, Germany

Tree network channels as fluid distributors constructing pyramidal polymer electrolyte fuel cells

Stephan M. Senn[a)] and Dimos Poulikakos[b)]

Swiss Federal Institute of Technology (ETH Zurich), Department of Mechanical and Process Engineering, Institute of Energy Technology, Laboratory of Thermodynamics in Emerging Technologies, ETH Zentrum, CH-8092 Zurich, Switzerland. (http://www.ltnt.ethz.ch)

ABSTRACT

In polymer electrolyte fuel cells, chemical energy of hydrogen is directly converted to electric energy. A proton-conductive polymer membrane separates the anode and cathode side of the cell where each side includes a fluid distribution system, a gas diffusion layer and a catalyst layer. Hydrogen is fed to the fluid delivery system on the anode side and diffuses through the gas diffusion layer to the catalyst layer where oxidation of hydrogen occurs. Protons are transported through the electrolyte phase of the catalyst layers and the membrane to react with oxygen in the cathode catalyst layer and to form water. Oxygen is fed to the cathode fluid delivery system, usually by means of humidified air, and it is subject to diffuse through the cathode gas diffusion or backing layer to the reaction sites in the cathode catalyst layer.

The cell performance is reduced as a result of the various loss mechanisms prevailing in the system. Reaction, activation, and concentration overpotentials are identified in the catalyst layers. Ohmic losses are due to electron flux in the backing layers, the catalyst layers and the current collector plates, and due to proton flux through the polymer electrolyte phase of the catalyst layers and the membrane. Concentration overpotentials in the catalyst layers are caused by reactant species depletion and mass transfer limitations between the bulk fluid flow in the channels and the reaction sites in the catalyst layers. The influence of mass transfer resistances depends on operating conditions, material properties of the backing layer, geometry parameters, and structural parameters. These include the size and the shape of the channel cross-sections, the topology of the fluid delivery system, the thickness, structure, porosity and permeability of the diffusion and catalyst layers, and the width of the current collector shoulders. Operating a cell at elevated temperature levels provides higher diffusivities for reactant and product species and hence reduces diffusion losses. At high current densities, substantial amount of liquid water may form on the cathode side, blocking pores in the backing layer and adding further resistance to mass transfer. In ribbed fluid distributors, diffusion paths from the channels to the reaction sites under the current collector shoulders are longer than the diffusion paths from the channels to the reaction sites straight under the channels. As a result, resistance to mass transfer between the channel and the part of the catalyst layer under the current collector shoulders is higher, causing increased concentration overpotential losses in these regions.

One-dimensional to fully three-dimensional mathematical models have been developed in the past and solved analytically or numerically to obtain a better understanding of the fundamental transport phenomena inside the fuel cell. While three-dimensional models provide the most instructive insight into the fundamental mechanisms occurring in the cell, today they still require substantial computational resources and computational time to be solved numerically with respect to entire cells. Multiparametric system optimization becomes even more expensive or impossible, especially if the number of optimization parameters within a certain objective function is large, requiring a lot of evaluations of the objective function. In contrast to three-dimensional models, one-dimensional models can usually be solved very fast, either numerically or even analytically, and therefore open the possibility to address complex multidimensional system optimization issues.

Multi-scale constructal tree-like channel networks (see FIG. 1) have been introduced [1-2] as a novel fluid distribution concept in polymer electrolyte fuel cells (PEFC and DMFC) and compared to traditional, non-bifurcating serpentine channel systems. The entire geometric structure of the tree network is optimized with respect to maximum electric power output and minimum flow resistance, subject to the

---

[a)] *E-mail: stephan.senn@ltnt.iet.mavt.ethz.ch*
[b)] *E-mail: dimos.poulikakos@ltnt.iet.mavt.ethz.ch*

constraint of a fixed cell area, leading to a deterministic tree network, which also defines the shape of the fuel cell (pyramidal or double-staircase shape). The corresponding multiparametric optimization problem is addressed by means of a genetic optimization algorithm (see FIG. 2).

In addition, a thorough multiphase model [3] for the porous diffusion layer of a polymer electrolyte fuel cell (PEFC) is presented that accounts for multicomponent species diffusion, transport and formation of liquid water, heat transfer, and electronic current transfer. Multiphase transport phenomena at decreasing length-scales (e.g., within a pyramidal PEM fuel cell) are then discussed. The governing equations are written in nondimensional form to generalize the results. The set of partial differential equations is solved based on the finite volume method. The algorithm was implemented in Fortran. Other contributions [4-6] and their relevance in this context are briefly mentioned.

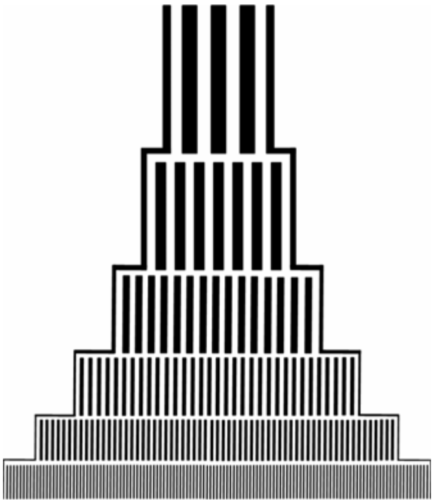

FIG. 1. Geometric structure of the tree network. Cut through the current collector flow-field. Channels (white) and current collector material (black).

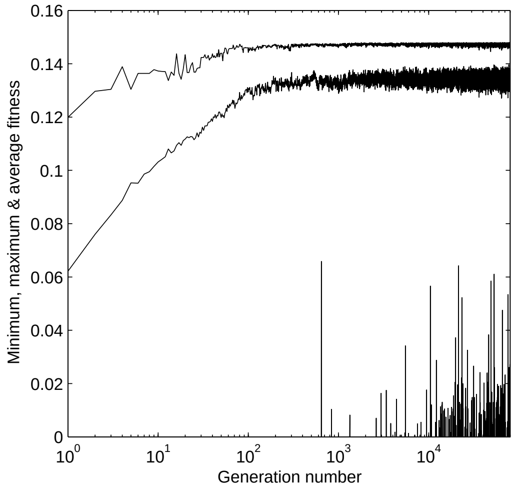

FIG. 2. Genetic optimization of the tree network. Maximum fitness (upper curve), average fitness (middle curve), and minimum fitness (lower curve). The fitness equals the net power density of the tree network.

ACKNOWLEDGMENT

This work was supported by the Swiss Federal Office of Energy (BFE) under contract no. 87100 (program manager Dr. A. Hintermann).

REFERENCES

[1] S.M. Senn, D. Poulikakos, “Tree network channels as fluid distributors constructing double-staircase polymer electrolyte fuel cells," *Journal of Applied Physics*, Vol. 96, No. 1, pp. 842-852, 2004.

[2] S.M. Senn, D. Poulikakos, “Pyramidal direct methanol fuel cells," *International Journal of Heat and Mass Transfer*, submitted for publication, 2004.

[3] S.M. Senn, D. Poulikakos, “Multiphase transport phenomena in the diffusion zone of a PEM fuel cell," *ASME Journal of Heat Transfer*, submitted for publication, 2004.

[4] S.M. Senn, D. Poulikakos, “Polymer electrolyte fuel cells with porous materials as fluid distributors and comparisons with traditional channeled systems," *ASME Journal of Heat Transfer*, Vol. 126, No. 3, pp. 410-418, 2004.

[5] S.M. Senn, D. Poulikakos, “Laminar mixing, heat transfer and pressure drop in tree-like microchannel nets and their application for thermal management in polymer electrolyte fuel cells,” *Journal of Power Sources*, Vol. 130, No. 1-2, pp. 178-191, 2004.

[6] S.M. Senn, D. Poulikakos, “Porous materials as fluid distributors in polymer electrolyte fuel cells – a computational performance analysis,” ASME International Mechanical Engineering Congress, Washington D.C., USA, November 16-21, 2003. Received the 2004 Best Student Paper Award by the ASME (American Society of Mechanical Engineers) Advanced Energy Systems Division (Systems Analysis Technical Committee).

Local Current Distribution over the Flowfield Ribs and Channels

Mathias Reum*, Stefan Freunberger, Felix N. Büchi

Electrochemistry Laboratory, Paul Scherrer Institut, CH-5232 Villigen-PSI

Abstract

In today's PEFCs, reactants generally are conducted over the active area in a channel and rib structure. This structure with lateral dimensions on the millimetre or sub-millimetre scale induces inhomgenieties in the local current density. This is due to liquid and gas transport restrictions and finite electronic conductivity in the porous structure of the gas diffusion media (GDL) employed.

These inhomogenieties generate voltage losses, which need to be understood and minimized. The problem has been approached by simulation i.e. [1]. However no systematic experimental results are available to validate the simulations.

For simulations the voltage drop in the GDL is a very important parameter. As the measurement in the real cell is difficult and error prone an approach for determination of the voltage losses in the backing using a non-electrochemical dummy cell is pursued (see Figure 1). This cell consists of a single real scale flow field channel and a dummy MEA realized by 0.1 mm metal stripes. The set-up allows for simulating of random current profiles over channel and rib of the flow field and determination of the respective electronic voltage drop in the GDL.

First results show, that the resistance in the backing for current generated over the channel is considerably different from that for current generated over the rib.

When similar resistance measurement will be made in real cells, the real current density will be accessible by solving the Laplace equation in the GDL with measured boundary conditions.

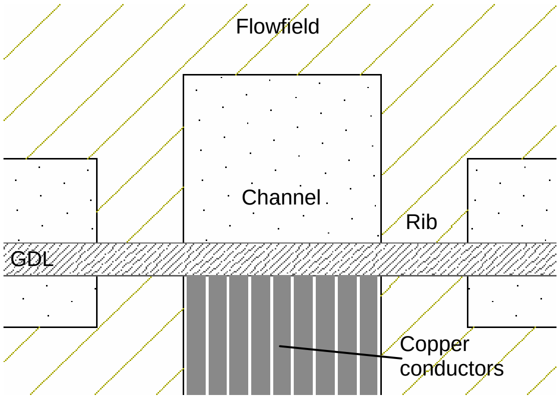

Figure 1: Dummy cell for experimental determination of anisotropic resistance in GDL as function of

[1] Hua Meng and Chao-Yang Wang, J. Electrochem. Soc., **151**, A385-A367 (2004)

*) mathias.reum@psi.ch / Tel.: +41 (0)56 310 2117

Electrical and Thermal
Cell-to-cell Coupling in PEFC Stacks

Stefan A. Freunberger[†,1], Felix N. Büchi[†], Nedjib Djilali[‡]

[†]Electrochemistry Laboratory, Paul Scherrer Institut, CH-5232 Villigen-PSI,
Switzerland

[‡]Institute for Integrated Energy Systems, University of Victoria, P.O. Box 3055,
Victoria, BC, V8W 3P6 Canada

Abstract

The bipolar arrangement in fuel cells stacks connects the individual cells electrically in series while the cells are connected in parallel for the reactant and coolant flows.

Therefore all cells in a stack have to carry the same total current while receiving reactant and coolant flows that are not perfectly equal due to varying percolation resistances. The local current production in a single cell will vary significantly with reactant flow rates and temperature distribution governed by the coolant flow and where applicable effects of the endplate. Due to the finite conductivity of the bipolar plates such local perturbations affect adjacent cells by impressing on them a similar current density distribution.

A 3-D CFD-model describing the effects of electrical and thermal coupling of PEM fuel cells through shared bipolar plates is developed. The numerical results show significant effects of anomalous reactant and coolant flow rates on adjacent cells and on the stack performance due to coupling. Since in general the current will flow through the stack following the path of least resistance – including charge transfer resistance in the electrochemical reaction and the resistance of the membrane – special attention is paid to the membrane model. Therefore a new mechanistic membrane model [1] is implemented that has been shown to match the experimental conductivities over the whole humidity and temperature range. Results with the new membrane model and established ones are compared.

Reference:

[1] J. Fimrite, B. Carnes, H. Struchtrup and N. Djilali, *submitted to the J. Electrochem. Soc.*

---

[1] Email: stefan.freunberger@psi.ch

Thermomechanical Simulation of SOFC-Stacks under Service

Jan Wenck, Axel Müller and Hubertus Michael Wigger
Universität Siegen, Institut für Mechanik und Regelungstechnik – Mechatronik, 57068 Siegen, Germany

Jochen Hebel, Wilfried Becker
Technische Universität Darmstadt, Fachbereich Mechanik, AG IV, 64289 Darmstadt, Germany

General survey

With the help of computer aided techniques, the analysis of the mechanical behaviour of single components of a high-temperature fuel cell stack or even the whole stack itself has become much easier. Therefore, modelling and simulation are appropriate tools for the study of the mechanical performance of SOFC-stacks under service conditions. The stack has to be calculated as a multimaterial composite system which has been preloaded by shrinking effects due to the manufacturing process. Inhomogeneous temperature fields during service cause additional internal stresses within the individual parts of the stack. As reason for these stresses which are considerable in some cases, the mismatch in the mechanical and thermal properties of the individual materials has to be named. In order to understand the thermomechanical behaviour of a fuel cell stack, the problem has to be approached by means of finite element analyses. After thorough investigation, the effects of the loads of the individual stack components are ascertained and the potential of mechanical optimization may be determined.
SOFC-stacks have to work reliably though they have to bear temperature loads of about 800°C during the heating up process and the subsequent cooling down from service temperature. Thus, the individual components of the stack are highly demanded, see Müller et al. 2002. Due to this, especially within the individual layers of multimaterial composite structures, like the membrane electrodes assembly (mea), internal stresses develop because the layers are not able to expand as free and unconstraint as if they were on their own. They are forced together as a composite laminate, thus obeying the same plane displacement field.

Theory

Inplane loaded plates are characterized as having a thickness *t* which is small in comparison with the other dimensions and are subjected to loads acting in the mid plane of the structure. All stresses are assumed to be distributed uniformly over the thickness independent of the transversal coordinate *z*. For isotropic materials, this state of plane stress is determined by a bipotential equation, for detailed information see Becker/Gross 2002, pp. 45, as follows

$$\frac{\partial^4\Phi}{\partial x^4}+2\frac{\partial^4\Phi}{\partial x^2\partial y^2}+\frac{\partial^4\Phi}{\partial y^4}=-E\alpha_T\left(\frac{\partial^2(T-T_0)}{\partial x^2}+\frac{\partial^2(T-T_0)}{\partial y^2}\right)-(1-\upsilon)\left(\frac{\partial^2 V}{\partial x^2}+\frac{\partial^2 V}{\partial y^2}\right)$$

with E as Young's modulus, α_T as the linear coefficient of thermal expansion (dependant on the temperature itself) and ν as Poisson's ratio. The Airy's stress function is given by Φ. T and T_0 represent the actual and the initial stress-free state temperature, respectively, while V denotes the potential of volume forces. Stresses from derivatives of Airy's stress function are

$$\sigma_{xx}=\frac{\partial^2\Phi}{\partial y^2}+V,\quad \sigma_{yy}=\frac{\partial^2\Phi}{\partial x^2}+V,\quad \tau_{xy}=-\frac{\partial^2\Phi}{\partial x\partial y}\,.$$

In the case of linear elastic material behaviour, the strains are related to the stresses through Hooke's constitutive law.

Structural analysis of the mea under different temperature loads

A structural analysis of the mea is performed using the finite element method. The mea is assumed to be of rectangular shape with free boundary conditions. The linear elastic behaviour is investigated with a focus on the electrolyte layer because this layer is assumed to be of primary interest when it comes to critical stress states and failure. Two different temperature loads are chosen to show their effects on the stress level of the electrolyte layer. The inplane stresses of the mea are considered as representative result quantities.

Linear temperature load

In order to assess the effect of spatial derivatives of the temperature distribution, the first temperature load *T* applied is chosen to be linear in the interval [-400; +400°C], see Figure 1. The structural response obtained by loading the mea with the linear temperature distribution is not a linear mapping of the temperature distribution. Only the thermal strain distribution reflects the temperature field, whereas the elastic strain corresponds to the field of the stress component σ_{11}. As can be seen in Figure 1, the stress distribution of σ_{11} shows a localization in the middle of the upper and lower boundaries of the mea. Furthermore, at the right boundary a concentration of tensile stress σ_{11} appears which has no compression counterpart of the same form at the opposite boundary. The stress localizations of the shear stress σ_{12} depicted in Figure 1, right, cannot be attained by purely intuitive assessment.

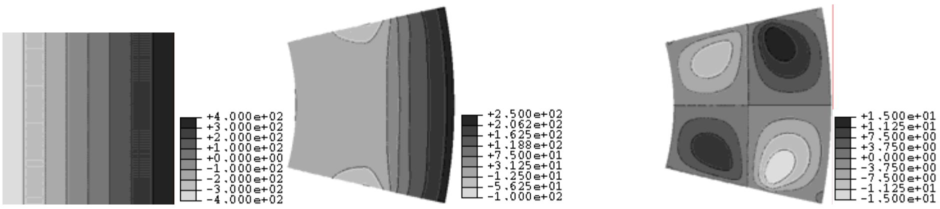

Figure 1: Linear temperature load, stress distribution σ_{11} (centre) and σ_{12} (right) in the electrolyte layer, deformed shape.

The stress distribution of the maximum principal stress σ_I, not shown here, shows a kind of affinity to the linear load distribution albeit there is also a stress localization near the right boundary. In the left part of the mea, the stress σ_I can surely not be concluded by simple intuitive assessment.

Radial quadratic temperature load

For the purpose of the assessment of the effect of higher spatial derivatives, the second temperature load is chosen to be described by the formula

$$T = 800\,°C \left(\frac{r}{r_0} \right)^2$$

and is therefore called radial quadratic temperature load, see Figure 2, left.

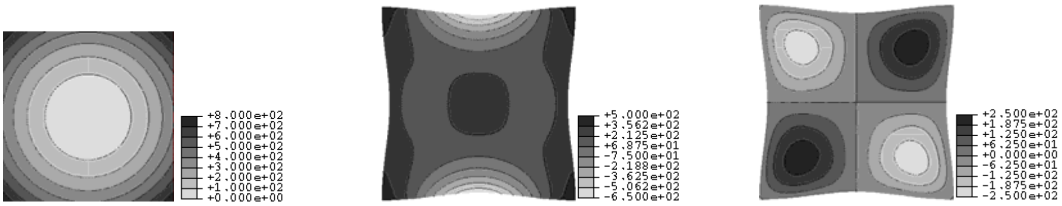

Figure 2: Temperature load with radial quadratic distribution, stress distribution σ_{11} (centre) and σ_{12} (right) in the electrolyte layer, deformed shape.

The response behaviour of the electrolyte layer for the radial quadratic temperature load cannot be intuitively obtained either. The stress distribution of σ_{11} in Figure 2, centre, reveals compressive stress localizations in the middle of the upper and lower boundaries of the mea as well as tensile ones at the corners of the structure. This Figure confirms point symmetry for the distribution of the shear stress σ_{12}. But this material response does not reflect the radial symmetry of the temperature load, particularly since the shear stress distribution as a result of a linear temperature load, Figure 1, is of similar kind.

Conclusions

Using the finite element method, the effects of spatial derivatives of a linear and a radial quadratic temperature load distribution on the electrolyte layer of the mea have been analyzed. It has been shown that the inplane stress distributions are neither trivial linear mappings of the applied loads nor that symmetric loading leads to symmetric structural responses of the same kind. Furthermore, stress localizations appear which cannot be concluded from just having the temperature load distribution at hand. This is due to the finite dimensions of the structure considered. The boundaries of the mea cause unexpected results which can not be obtained intuitively. Therefore, it is reasonable and required to perform analyses like the present one to gain further insight into the structural behaviour of the mea under temperature loading.

References

Becker/Gross 2002 — Becker, W.; Gross, D.: *Mechanik elastischer Körper und Strukturen*, Berlin · Heidelberg · New York, Springer-Verlag, 2002.

Müller et al. 2002 — Müller, A.; Hohe, J.; Becker, W.; Stolten, D.; de Haart, L. G. J. (Bert): *Structural stress and sensitivity analysis revealing optimization potential of SOFC stacks.* In: Huijsmans, J. (ed.): 5th European Solid Oxide Fuel Cell Forum, Vol. 2, European Fuel Cell Forum, Switzerland, 2002, pp. 791–798, 2002.

Acknowledgements

The authors are grateful to the IWV 3 of the german Forschungszentrum Jülich – chiefly D. Stolten and L. G. J. (Bert) de Haart – for financial support and fertile cooperation.

Proceedings
2^{nd} Fuel Cell Research Symposium - Modelling and Experimental Validation
March 3-4, 2005, German Aerospace Center, Stuttgart, Germany

Effects of microreactor wall conduction on the reforming process of methane

Michael J. Stutz, Claudio Iseli and Dimos Poulikakos

Laboratory of Thermodynamics in Emerging Technologies, Institute of Energy Technology,
Department of Mechanical and Process Engineering, Swiss Federal Institute of Technology Zurich,
ETH Zentrum, CH-8092 Zurich, Switzerland.

ABSTRACT

There has been a significant interest in recent years in fuel processing that provides syngas (hydrogen and carbon monoxide) for Fuel Cells. One important syngas production route is autothermal reforming, which combines catalytic partial oxidation (POX), steam reforming (SR), the water gas shift reaction (WGS) and dry reforming (DR). It is considered to be thermally self-sustaining, and therefore, does not produce or consume external thermal energy. Catalysts are commonly used to enhance the reaction rate of the reforming processes at lower temperatures [1].

Numerical modeling is a powerful tool to give a better understanding of the fundamental transport phenomena inside the reformer and it is extremely useful in sizing the reactor, in setting the operating conditions and in predicting the dynamic effect of operating conditions [2]. Inlet flow temperature, mass flow rate and mixture composition strongly influence the syngas yield and the soot formation, which is a big problem in reactor operation because it deactivates the catalyst and therefore leads to a lower overall efficiency [3].
Transport phenomena in a channel based reformer can be described by the conservation equations of mass, momentum, energy and species leading to a set of non-linear partial differential equations (PDE). The channel flow is always considered laminar. A single channel with all adiabatic walls is modeled in steady state conditions, which is a good representation of the conditions in a fully isolated single-channel reactor and also a good approximation for a monolith reactor [4].
The fluid is assumed to be an ideal gas mixture which follows Dalton's model. The specific enthalpy of an ideal gas mixture is approximated using the JANAF tables and are dependent on temperature only. The momentum conservation equation neglects all body forces but includes pressure and viscous effects. The mixture is assumed to be a Newtonian fluid. Neglected in the shear stress tensor is the bulk viscosity. The local dynamic viscosity is established based on the Chapman-Enskog theory for multi-component gas mixtures at low density [5]. The steady state conservation equation of energy excludes body forces and viscous dissipation but considers heat flux and compression work. The heat flux term accounts for thermal conduction, computed by the Mix Kinetic Theory [5], and energy transport by species diffusion. The steady state species conservation equation does not consider source terms, because no homogeneous reaction is assumed to take place at atmospheric pressure and usual operating temperatures of a methane reformer [6]. The species flux is composed of a concentration driven and a thermal diffusion term but the pressure diffusion is neglected. The concentration driven diffusion coefficient is obtained from the Chapman-Enskog theory .
All surface reactions are specified using a detailed multi-step finite-rate reaction mechanism with 7 gas phase species, 12 site species and 38 elementary surface reactions. The reaction rate coefficients are expressed by the semi-empirical Arrhenius equation, the adsorption mechanism is computed by the sticking coefficient method. The boundary condition at the catalytic surface is defined by a species flux balance.

The micro-scale channel reactor of the numerical simulations is represented by a cylindrical tube of 1mm diameter and 10mm length covered with Rhodium. The inlet gas is a mixture of methane in dry air with a C/O ratio of 0.7. Two different models have been used that are both radially symmetric. The first model consists of only one domain, namely the channel with an adiabatic wall, where the surface reaction takes place. This modeling approach has already been used by Chaniotis and Poulikakos [7]. The second model is composed of two domain, the channel and the thermally conductive channel wall made of aluminum cordierite. The boundary conditions for the walls are all adiabatic, except for the interface between channel and wall, where the catalytic reaction occurs.

To numerically solve the coupled set of partial differential equations, a finite-volume central scheme is used. The licensed solver is called CFD-ACE distributed by CFDRC of Huntsville, USA. The surface

reaction boundary condition is solved by the coupled Newton-Raphson method [8].

The temperature profiles can be calculated at different positions inside the tubes for the model that does not take into account the channel wall axial conduction (No-wall-model) and the one considering this effect (Wall-model). The wall temperature rises monotonically in the streamwise direction to a maximum temperature of 1735 K, lying 1.2 mm behind the inlet of the No-wall-model. The maximum wall temperature of the Wall-model is 1439 K, thus significantly lower. Its location, that is 1.1 mm behind the inlet, slightly more upstream compared to the no wall model [*Fig. 1*].

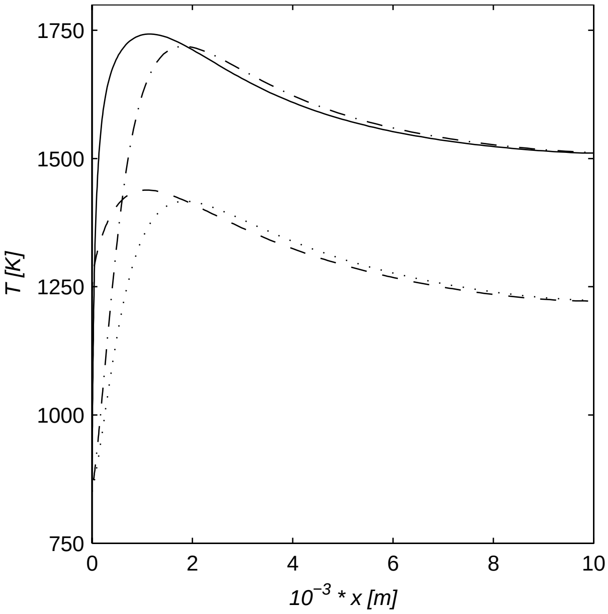

Fig. 1: Mixture temperature along centerline (-.-), and at channel wall (–) of the No-wall-model. Mixture temperature along centerline (···), and at channel wall (- -) of the Wall-model.

The steep rise of the wall temperature right behind the inlet is due to the strongly exothermic total oxidation on the catalyst surface. The fuel conversion of the No-wall-model is always higher than the one of the Wall-model. Therefore more Methane is totally oxidized in the No-wall-model, which explains the higher temperature along the channel. Farther downstream the wall temperature decreases monotonically, thus the endothermic reactions prevail. The gas mixture temperature curve along the centerline has a similar shape as the wall temperature curve but it is shifted to the right due to species transport.
Methane conversion and hydrogen yield are important characteristics that illustrate fuel processing efficiency. High fuel conversion and high syngas yield are decisive in reactor design. In *Fig. 2* the hydrogen yield and the methane conversion are plotted in flow direction. 97% of methane is converted in the No-wall-model at the outlet, which is 8% more than the methane conversion of the Wall-model. The hydrogen yield comes up to 79% for the No-wall-model, which is 9% higher than the calculated value for the Wall-model.

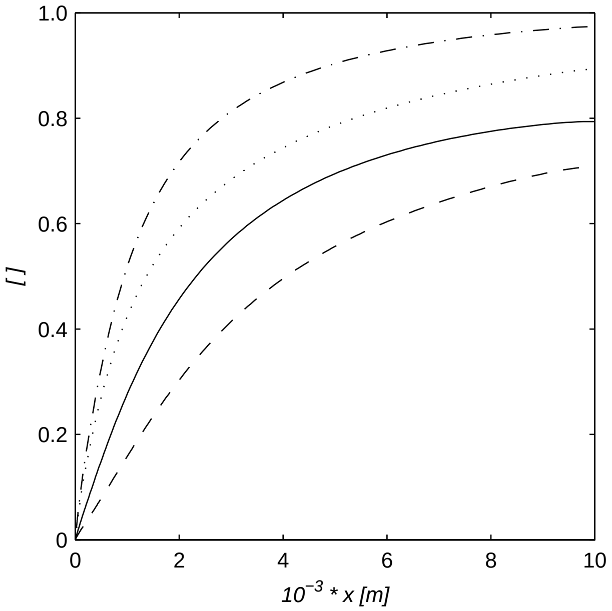

Fig. 2: Hydrogen yield (–) and methane conversion (-.-) in flow direction of the No-wall-mode. Hydrogen yield (- -), and methane conversion (···) of the Wall-model.

It is clearly shown that the wall axial conductivity plays a major role in the reforming reactions. Neglecting the wall effects leads to significantly higher channel temperatures and overpredicts hydrogen yield and methane conversion.

ACKNOWLEDGEMENTS

Financial support for this work provided by the Bundesamt für Energie (BfE) of Switzerland under the direction of Dr. A Hintemann is gratefully acknowledged. The preceding work by Dr. A. K. Chaniotis is also thankfully acknowledged.

REFERENCES

[1] H. Jung, W.L. Yoon, H. Lee, J.S. Park, J.S. Shin, H. La, J.D. Lee, *J. Power Sources*. **2003**, 124(1), 76-80.
[2] J. Mantzaras, C. Appel, P. Benz, *Proc. Combust. Inst.* **2000**, 28, 1349-1357.
[3] C.T. Goralski, R.P. O'Connor, L.D. Schmidt, *Chem. Eng. Sci.* **2000**, 55(8), 1357-1370.
[4] R. Schwiedernoch, S. Tischer, C. Correa, O. Deutschmann, *Chemical Engineering Science*. **2003**, 58(3-6), 633-642.
[5] R.B. Bird, W.E. Stewart, E.D. Lightfoot, *Transport Phenomena*, John Wiley & sons, New York 1980.
[6] O. Deutschmann, L.D. Schmidt, *Aiche J.* **1998**, 44(11), 2465-2477.
[7] A.D. Chaniotis, D. Poulikakos, *J. Power Sources*. **2005**, in press.
[8] S. Mazumder, S.A. Lowry, *J. Comput. Phys.* **2001**, 173(2), 512-526.

Dynamic Modelling of PEMFC Stacks using MATLAB-Simulink

A. Vath, M. Söhn, N. Nicoloso, and Th. Hartkopf

Technische Universität Darmstadt
Institut für Elektrische Energiesysteme
Landgraf-Georg-Str. 4,
D-64283 Darmstadt, Germany

Fuel cell technology plays an important role in the development of alternative energy converters for mobile, portable and stationary applications. Modelling (and validation) of fuel cell components and entire systems opens new ways for the design of fuel cells and the investigation of their stationary and dynamical behaviour. In this work Proton Exchange Membrane Fuel Cell (PEMFC) Stacks, typically comprising 5 to 50 cells, are dynamically modelled within MATLAB-Simulink at various operation conditions in order to establish a comprehensive fuel cell description and to explore the modelling facility as a diagnostic tool.

A one dimensional stack model is used to describe the different layers of each cell with their physical and electrochemical characteristics. The gas diffusion layer is modelled as a porous media, usually made out of carbon fibres. Here it is necessary to include the amount of liquid water since the pores may get filled with water slowing down the diffusion of the fuel. In the diffusion and catalyst layer the transport mechanism of hydrogen, nitrogen, oxygen, water vapour and liquid water are incorporated. Other processes investigated by the dynamic 1D model include, e.g., the membrane resistance as a function of the water content during fast load changes/production of water at cathode side. The water transport through the membrane considers the effects of concentration gradients and the electro-osmotic drag. The nitrogen and hydrogen transport through the membrane are also included. The stack used for verification of the results was water cooled and the gases at the inlet of this stack humidified during the measurement to see the influence of the membrane resistance during operation. The main relations incorporated for the calculation of the cell voltage are the current density, partial pressure of the gases in the catalyst layers, the membrane resistance, double layer capacity at the cathode, the exchange current density, the temperature, etc..

The dynamic behaviour of the stack with homogeneous cells is simulated and compared with the experiment. Main emphasis has been given to the time dependent effects of membrane humidifying/drying, temperature and flow rate. In the following typical results of the 1-D dynamical fuel cell model are shown (Figs. 1 and 2). The gases at the inlet of this stack have not been humidified during the measurement to see the influence of the membrane resistance during operation more clearly.

In Figure 1 the calculated cell voltage is compared with the measured values for dynamical loads. There is excellent agreement between the simulation and the experiment. The next figure shows the calculation of the different potential changes at cathode, anode and membrane and of the entire cell voltage. The cathode potential change has quite the same characteristic as the current density shown in Figure 2. The change of the anode potential follows the cathode potential change but its amplitude is very low (by a factor of 10^2 - 10^3). The membrane potential change depends on the current density and the proton conductivity.

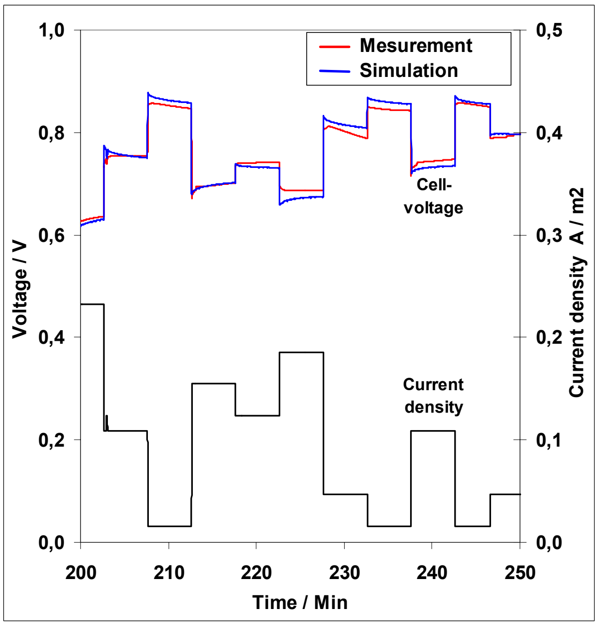

Fig. 1: Comparison of Simulation/Experiment

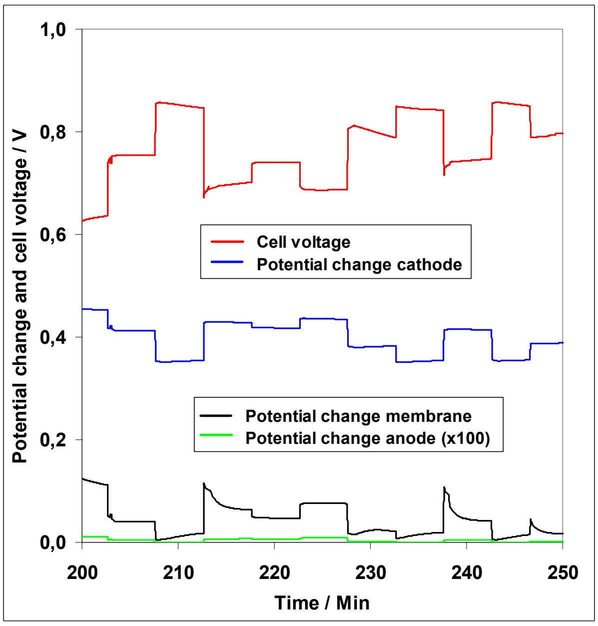

Fig. 2: Potential Changes at Dynamic Operation

The model is also capable of describing the transient features occurring in U(t)- and I(t)- curves. The change in cell voltage mainly depends on two effects. After a current step the anode/cathode charging (double layer capacity) approaches its new equilibrium value within the first seconds. The change of the membrane properties (water content, proton conductivity) is, however, far slower and determines the dynamics. This effect depends on the membrane thickness, temperature, etc. and therefore gets more pronounced under extreme working conditions (high loads steps at dry membrane conditions) which often decrease performance and lifetime. With the help of the modelling results such unfavourable conditions have been analysed and will be discussed in more detail.

Currently we explore the capabilities of modelling to establish the relevant control parameters for intelligent control programs improving operational stability and efficiency. To this end, the model has been used to describe the influence of inhomogeneities in the stack, e.g., by temperature gradients, lower medium flow in one cell, etc, since cells with poor performance reduce the stack performance to various degree. This feature will be especially helpful for the quality assurance and long term stability check.

Requirements on PEFC system modelling used in the development of automotive propulsion systems

Peter Treffinger, Deutsches Zentrum für Luft- und Raumfahrt
Pfaffenwaldring 38-40 - 70569 Stuttgart, Germany
Tel +49 711 685 7468 - Fax +49 711 685 7465
peter.treffinger@dlr.de

Despite of continuing efforts on modeling the status of the available models and tools is still subject of a broad discussion in the literature:

Haraldsson and Wipke [HAR2004] give an overview of PEFC system models. The models were realized predominantly on the basis of the simulation environment Matlab/Simulink. Haraldsson and Wipke stated that the experimental validation of the models is rather poor. Additionally none of the models fulfilled the requirements: dynamic model, fuel cell stack model with heat and water management, incorporation of fluid dynamics in the cathode and anode feed, thermal properties, which permit evaporation and condensation, ability to be integrated into a vehicle model.

Yao et al. [Yao2004] give an overview of the status of PEFC stack models. The authors state that the description of individual phenomena e.g. mass transfer in the gas diffusion layer has made significant progress. However, they mention also that model validation should be improved and two-phase-flow effects should be included as well as effects of the gas dynamics.

System modeling is an important tool developing automotive propulsion systems. However, DLR made in a vehicle development project the experience that the requirements on fuel cell stack models to be used for practical work differ in some aspects from the main stream, which is discussed in the literature.

Based on the experience of the HyLite project the requirements on fuel cell system models for the usage in practical system development will be explained in the presentation. There are several issues to consider when designing a fuel cell system for automotive application, e.g. sufficient dynamic of the system, water-neutrality, high efficiency of the system (Which is a main argument for fuel cell powered propulsion!), and ability to extract sufficient power also under cold-start conditions. The issues mentioned above are partly contra dictionary, e.g. system dynamics and efficiency. Within the HyLite project it turned to be out that experiments are still essential as basis for the system design. This finding will be illustrated within the presentation by experimental results on the dynamic behaviour of the fuel cell system, which is essentially for the design of the control system. For instance the maximum step in current, which could be applied to the fuel cell system of the HyLite vehicle was not limited by the dynamics of the supply system or the dynamics of the stack itself. The limiting factor was the non-uniformity of the single-cell-voltage, namely some weak cells, which reached the minimum voltage allowed.

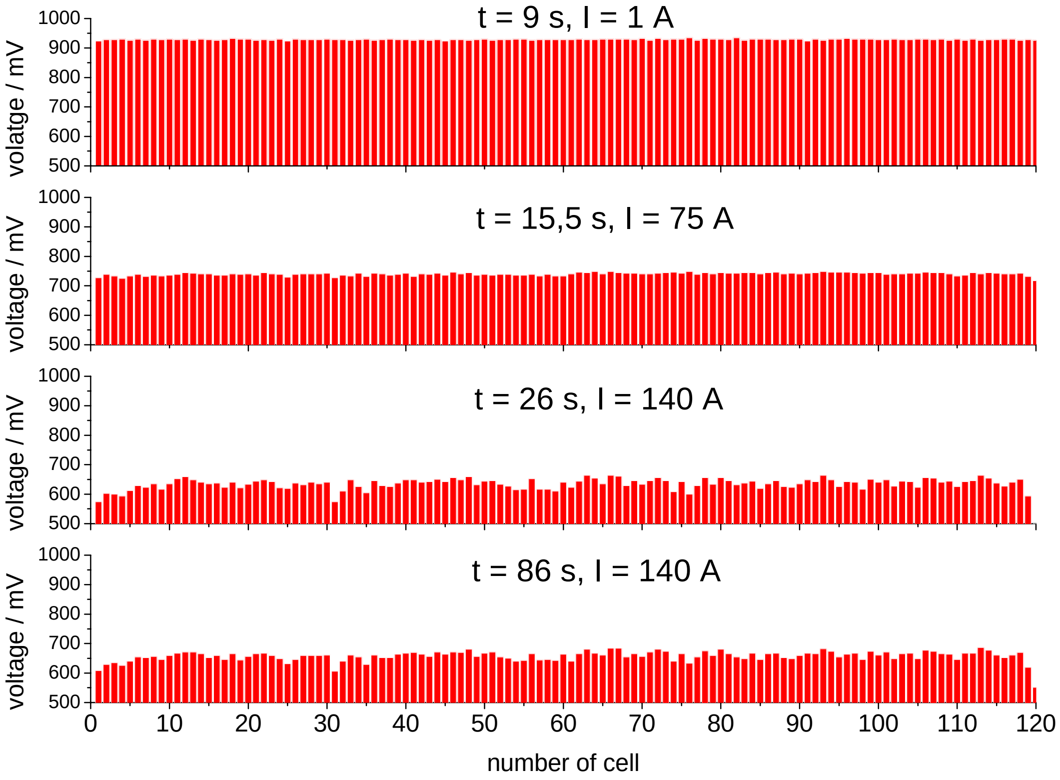

Fig. 1: Single-cell voltage as a function of time during the full load test described in figure 4. Results for a „full load“ test, i.e. rapid current increase up to the maximum current following the operating strategy A (mass flow rate of air and cathode pressure follow the load).

The figure shows the development of the single cell voltages during a current step from 0 to 140 A, whereby a load following strategy has been applied. It can be seen that the non-uniformity – an effect, which is difficult to consider in stack modelling -increases drastically from 75 A to 140 A.

Literature

[HAR2004]	Haraldsson, K, Wipke, K: Evaluating PEM fuel cell system models, Journal of Power Sources 126 (2004) 88–97
[Yao2004]	Yao, K.Z. et al: A review of mathematical models for hydrogen an direct methanol polymer electrolyte membrane fuel cells, FUEL CELLS 4(2004) 3-29

Investigation of Gas Diffusion in Fuel Cells under Operating Conditions

Nicola Bundschuh, Birgit Thoben
German Aerospace Centre
Institute of Technical Thermodynamics
Pfaffenwaldring 38 – 40
D-70569 Stuttgart

Abstract

The nature of the porous media and their influence on fuel cell performance is of key interest in optimizing the PEFC and SOFC. Coming from the flow field, the reactants must cross the porous media to reach the catalyst layer. Therefore, the ability of the gaseous and liquid reactants to access the catalyst will partly depend on the diffusion properties of the porous media. The most obvious questions in addition to a sufficiently detailed modelling and characterization of the fuel cell can be found in liquid and gas distribution and their transport through the porous media. Since the diffusion coefficient of reactants in porous media is a key parameter and due to the complexity of the porous media structure, it is necessary to determine the effective diffusion coefficient of the reactants experimentally. A test rig has therefore been build up to measure the effective gas diffusion coefficient. The rig contains a diffusion cell according to Wicke [1], which consists of two chambers separated by the investigated porous media.

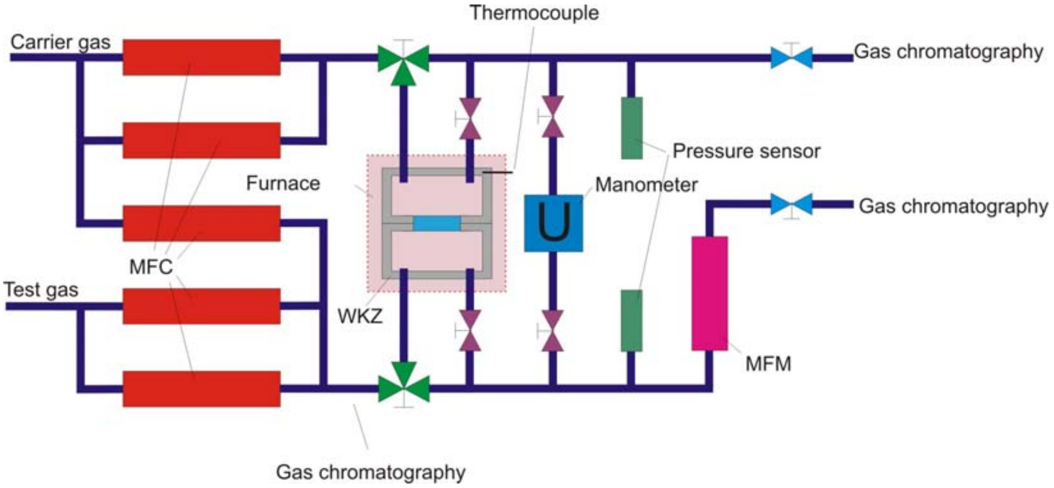

Figure 1: Concept of the test rig

The pressure difference between the chambers is set to zero. Well defined gas flows through each chamber pass the surface of the investigated sample. With a gas chromatograph it is possible to determine the composition of the gas flow at the in- and outlet of each chamber and thus determine the diffusive fluxes through the sample. The Wicke-Kallenbach diffusion cell (WKZ in fig. 1) is positioned in a furnace to reach the desired temperature range. Mass flow controllers (MFC) with different flow ranges are used to set different concentration gradients across the porous layer (in the centre of WKZ in fig. 1). A U-pipe filled with water delivers the differential pressure over the diffusion chamber. The absolute pressure in the feeding lines is given from commercial pressure sensor.

Modelling the gas transport through porous media, the effective diffusivity is usually calculated from the Stefan-Maxwell diffusion coefficient by

$$Deff = \frac{\varepsilon}{\tau} Dij$$

Combining D_{eff} from the Wicke-Kallenbach experiment for dry gases with the porosity ε measured by mercury porosimetry an experimentally determined value for the parameter τ is gained from the above equation. τ comprises all factors inhibiting species transport within the porous media like indirections and dead-end pores.

For validation of the measurements the flow field inside the diffusion chamber is modelled with the CFD-code “StarCD”. The porous media are regarded as permeation resistance and molecular gas diffusion takes place through the porous layers. Figure 2 shows the concentration distribution of oxygen in nitrogen with an inflow concentration of 10%

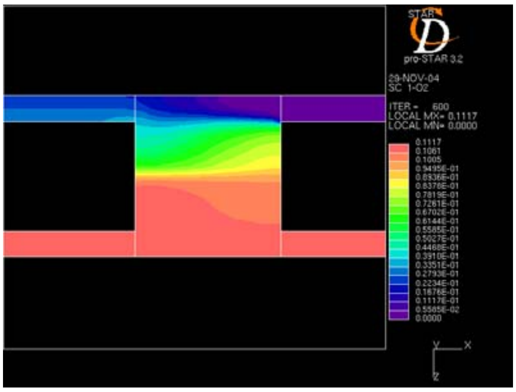

Figure 2: Concentration distribution inside the diffusion chamber

The results of the simulation show, that the circular design of the Wicke-Kallenbach diffusion cell works very well and there is no negative influence of the geometry on the flow.

Measurements of the effective diffusion coefficients of different gas diffusion layers for PEM fuel cells at room temperature and of the support layer and the porous electrodes of SOFC produced after the DLR-VPS-design from room temperature up to1073 K have been done. In figure 3 as an example some effective diffusion coefficients of hydrogen for different PEM gas diffusion layers are shown. The investigated materials are a metal filter (filter) as reference material and the following gas diffusion layers: From ETEK: Solid Polymer Electrolyte Electrode (ELAT®) V2 hand fabricated single side coating without catalyst (Single Sided V2), Carbon Cloth A, Solid Polymer Electrolyte Electrode (ELAT®) V2 hand fabricated double side coating without catalyst (Double Sided V2) and from SGL: Gas diffusion layer with 5% PTFE and on one side micro porous layer (GDL 30 BC).

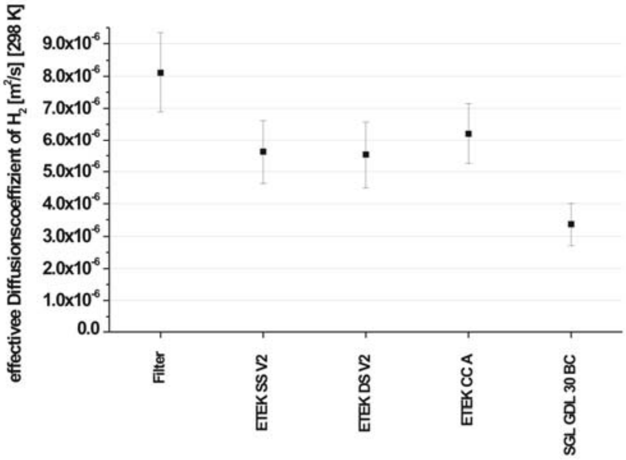

Figure 3: Effective diffusion coefficients for different PEM gas diffusion layers

One can see, that the effective diffusion coefficients differ not much from the ETEK materials. The measurements uncertainties are mainly influenced by the quality of the calibration gas mixture used by the gas chromatography.

A Simulation has also been done to get information about the pore structure and the morphology of the porous media. A single cylindrical pore of a PEM cathode is regarded in high current density conditions. The inlet conditions of relative humidity and the pore length are varied and the electrochemical kinetic is studied in dependence of different boundary conditions.

[1] Wicke, E., Kallenbach, R.: Die Oberflächendiffusion von Kohlendioxid in aktiven Kohlen. Kolloid-Zeitung Band 97, Heft 2, S. 135-151, 1941